haematologica
Journal of the Ferrata Storti Foundation

CSF1R modulates megakaryopoiesis by targeting RUNX1 in immune thrombocytopenia

by Haohao Han, Meng Zhou, Jiaqian Qi, Xiaofei Song, Xueqian Li, Ziyan Zhang, Tingting Pan, Xiaoyan Xu, Mengting Guo, Depei Wu and Yue Han

Received: July 1, 2025.
Accepted: December 12, 2025.

Citation: Haohao Han, Meng Zhou, Jiaqian Qi, Xiaofei Song, Xueqian Li, Ziyan Zhang, Tingting Pan, Xiaoyan Xu, Mengting Guo, Depei Wu and Yue Han. CSF1R modulates megakaryopoiesis by targeting RUNX1 in immune thrombocytopenia.
Haematologica. 2025 Dec 18. doi: 10.3324/haematol.2025.288511 [Epub ahead of print]

CSF1R modulates megakaryopoiesis by targeting RUNX1 in immune thrombocytopenia

Haohao Han[1,2,3]*, Meng Zhou[1,2,3]*, Jiaqian Qi[1,2,3]*, Xiaofei Song[1,2,3], Xueqian Li[1,2,3], Ziyan Zhang[1,2,3], Tingting Pan[1,2,3], Xiaoyan Xu[1,2,3], Mengting Guo[1,2,3], Depei Wu[1,2,3#], Yue Han[1,2,3,4#]

[1]National clinical research center for hematologic diseases, Jiangsu Institute of Hematology, The First Affiliated Hospital of Soochow University, Suzhou, China.

[2]Institute of Blood and Marrow Transplantation, Collaborative Innovation Center of Hematology, Soochow University, Suzhou, China.

[3]Key Laboratory of Thrombosis and Hemostasis of Ministry of Health, Suzhou, China.

[4]State Key Laboratory of Radiation Medicine and Protection, Soochow University, Suzhou, China.

*HHH, MZ, and JQQ contributed equally to this study.

[#]Corresponding Author

Yue Han, MD, PhD, The First Affiliated Hospital of Soochow University, Jiangsu Institute of Hematology, 188 Shizi Street, Suzhou, Jiangsu province, People's Republic of China 215006. Email: hanyue@suda.edu.cn, Tel: +86 13901551669.

Depei Wu, MD, PhD, The First Affiliated Hospital of Soochow University, Jiangsu Institute of Hematology, 188 Shizi Street, Suzhou, Jiangsu province, People's Republic of China 215006. Email: drwudepei@163.com, Tel: +86-0512-67781856.

Author Contribution

YH and DPW conceived and supervised the study. HHH, MZ and JQQ performed experiments, analyzed data, and drafted the manuscript. XFS, XQL, ZYZ, TTP, XYX, and MTG contributed to experiments and data analysis. All authors read and approved the manuscript.

Running head

CSF1R modulates megakaryopoiesis in ITP.

Data-sharing statement

All original data can be provided if necessary. The raw single cell sequencing data generated in this study have been deposited in the Gene Expression Omnibus (GEO) database under

accession number GSE275370.

Funding

This work was supported by the National Natural Science Foundation of China (82230005, 81873432, 82200133, 82200137 and 82070143), grants from the Elite Talent Reserve Program of the First Affiliated Hospital of Soochow University and Jiangsu Province of China (BE2021645), Translational Research Grant of NCRCH (2021ZKMA01 and 2021ZKQA01) and the Priority Academic Program Development of Jiangsu Higher Education Institutions (PAPD).

Disclosures

The authors declare no competing financial interests.

Patient consent statement

Written informed consent was obtained from all participants.

Ethics statement

All research programs are in line with the guidelines of the Ethics Committee of Soochow University and follow the Declaration of Helsinki.

Abstract

Immune thrombocytopenia (ITP) is an autoimmune bleeding disorder characterized by platelet destruction and defective megakaryopoiesis. However, the mechanisms underlying megakaryocyte (MK) dysfunction in ITP remain unclear. To address this, we performed single-cell RNA sequencing (scRNA-seq) on bone marrow cells from a newly diagnosed ITP patient. ScRNA-seq analysis revealed a marked upregulation of *colony-stimulating factor 1 receptor (CSF1R)* in MKs compared with healthy control. This finding was independently validated by flow cytometry in additional clinical samples. In vitro, MK differentiation and maturation were significantly impaired in ITP, and these defects were rescued by inhibition of CSF1R. In an active murine model of ITP, CSF1R inhibition accelerated platelet recovery. Mechanistically, elevated CSF1R expression suppressed the transcription factor RUNX1, a key regulator of megakaryopoiesis. In conclusion, our findings identify CSF1R as a previously unrecognized regulator of megakaryopoiesis and suggest it as a promising therapeutic target in ITP.

Key words

Immune thrombocytopenia (ITP), colony-stimulating factor 1 receptor (CSF1R), megakaryocyte (MK), megakaryopoiesis, RUNX1

Introduction

Immune thrombocytopenia (ITP) is an autoimmune bleeding disorder characterized by isolated thrombocytopenia, yet its precise pathogenesis remains elusive. Traditionally, ITP has been attributed to antibody-coated platelets that are cleared primarily by macrophages in the spleen via interactions with Fcγ receptors and complement receptors[1-3]. Desialylated platelets mediated by antibody can also be cleared in the liver[4, 5]. Additionally, cytotoxic T-lymphocytes ($CD8^+$) not only destroy autologous platelets via apoptosis and perforin/granzyme-mediated cytotoxicity[6], but also induce platelet desialylation, thereby promoting hepatic clearance[7].

However, growing evidence indicates that, beyond the excessive immune-mediated platelet destruction, defective maturation of megakaryocytes (MKs) also plays a pivotal role in the pathogenesis of ITP[2, 8]. Megakaryopoiesis is a highly regulated and complex process within the bone marrow (BM), beginning with the lineage commitment of hematopoietic stem cells (HSCs) toward megakaryocytic progenitors (MKPs). These progenitors undergo multiple rounds of endomitosis to form MKs, which subsequently extend proplatelets and release platelets into the bloodstream[9, 10]. Several factors contribute to the defective MK differentiation and platelet production in ITP. For instance, MKs express platelet-specific glycoproteins such as GPIIb/IIIa and GPIb/IX[11-13], which serve as targets for autoantibodies in ITP patients. These antibodies not only promote platelet clearance but also impair MK maturation, leading to reduced MK numbers and defective platelet production[14, 15]. In addition, impaired MK apoptosis mediated by cytotoxic T lymphocytes, as well as abnormalities in the BM microenvironment, including mesenchymal stem cell dysfunction, dysregulated cytokine profiles, and reduced thrombopoietin (TPO) levels, have also been associated with decreased megakaryopoiesis[10, 16]. Therefore, therapeutic stimulation of MKs has become a key strategy to elevate platelet counts in ITP patients. TPO receptor agonists (TPO-RAs), such as eltrombopag and romiplostim, significantly enhance platelet production and achieve sustained responses in a substantial proportion of patients[8, 17, 18]. Nevertheless, in some patients, resistance or intolerance to TPO-RA occurs due to adverse events, including thrombosis, hepatotoxicity, or progressive BM fibrosis, manifested by increased reticulin

levels[19-21]. These limitations highlight the urgency to further explore alternative molecular pathways involved in MK dysfunction in ITP.

The colony-stimulating factor 1 receptor (CSF1R, CD115) is an essential receptor tyrosine kinase predominantly expressed on various myeloid cells. It plays a central role in regulating cell survival and function via interaction with its ligands, macrophage colony-stimulating factor (M-CSF) and interleukin-34 (IL-34)[22]. Beyond its established function in monocytes and macrophages, CSF1R is also moderately expressed in HSCs, common myeloid progenitors, and common lymphoid progenitors, indicating its broader involvement in early hematopoietic development[23, 24]. Importantly, CSF1R expression has also been identified in MKs[25, 26]. Grabert et al[25] used CRISPR-Cas9 gene editing to create a CSF1R-T2A-FRed knock-in mouse model, in which a fluorescent reporter was fused to the C-terminus of CSF1R; they found that CSF1R-FRed is expressed not only in monocytes and macrophages but also in MKs and $CD41^+$ progenitors within mouse BM. Consistently, Cortegano et al[26] reported that $CD45^{++}CD11b^+CD115^+$ ($CSF1R^+$) embryonic progenitors can give rise not only to myeloid/monocytic cells but also to a small population of immature adult-type $CD45^+$MKs. In adult C57BL/6 mice, approximately 26% of BM MKs ($Ter119^-CD45^+CD9^{++}CD41^{++}CD42c^+$) express CSF1R, reflecting the biological heterogeneity of MK developmental pathways. However, the functional role of CSF1R in MKs remains unclear. Whether CSF1R directly regulates MK differentiation and maturation, and the underlying mechanism, is still unknown. In this study, we identified aberrantly increased CSF1R expression in the BM of ITP patients. We further demonstrate that CSF1R impairs MK maturation by downregulating the transcription factor RUNX1, thereby contributing to the defective thrombopoiesis in ITP.

Methods

Patient Samples

Single-cell RNA sequencing (scRNA-seq) was performed on BM cells from a newly diagnosed ITP patient and a matched healthy donor (HD) at the First Affiliated Hospital of

Soochow University to identify subset-specific gene expression changes (Supplementary Methods). Cell clusters were annotated using specific marker genes reported previously (Table S1). For validation, BM samples from 26 ITP patients and 18 HDs (clinical characteristics summarized in Tables S2) were used. Levels of CSF1R ligands (M-CSF and IL-34) were measured by enzyme-linked immunosorbent assay (ELISA) in BM (26 ITP, 18 HDs) and peripheral blood (30 ITP, 20 HDs) samples, with patient characteristics summarized in Tables S3-S4. Detailed inclusion and exclusion criteria for ITP are provided in the supplementary methods. The study was approved by the Ethics Committee of the First Affiliated Hospital of Soochow University, and informed consent was obtained from all participants.

Cell Culture and Treatment in Vitro

$CD34^+$ cells were extracted from the HD peripheral blood mononuclear cells using the EasySep Human CD34 Positive Selection Kit (Stem Cell Technologies, Canada) via immunomagnetic separation. Purified cells were seeded at 1×10^5 cells/well in Stem Span SFEM II medium (Stem Cell Technologies, Canada) supplemented with 100 ng/mL TPO, 100 ng/mL stem cell factor (SCF), and 10 ng/mL interleukin-3 (IL-3) (Pepro Tech, USA) to induce MK differentiation[27]. Cultures were maintained for 10-12 days, with 50% medium replaced on days 4, 7, and 10, and 1% fresh plasma from ITP patients or HDs was supplemented at each change to maintain plasma-derived factors. Cytokine dynamics were monitored during the first 4 days after plasma addition (Supplementary Methods). The CSF1R inhibitor (cFMS Receptor Inhibitor II, 2 μM; MCE, USA) was added on days 0, 4, and 7 and maintained throughout differentiation. Details of inhibitor validation are provided in the Supplementary Methods.

Active Mouse ITP Model and CSF1R Inhibition

Wild-type (WT) C57BL/6N mice were obtained from the Laboratory Animal Center of Soochow University and heterozygous CD61 knockout ($CD61^{+/-}$) mice on the same background were kindly provided by Dr. Yi Wu (Soochow University, China). Animal

experiments were approved by the Animal Ethics Committee of Soochow University.

An active ITP model was established by transfusing $CD61^{-/-}$ mice weekly with 1.5×10^8 WT platelets for 6 weeks, as previously described[28] with minor modifications. Splenocytes (1×10^7 cells) from immunized $CD61^{-/-}$ mice were transferred into WT recipients to induce ITP [29, 30]. To assess the effect of CSF1R inhibition, mice received oral administration of the CSF1R inhibitor (cFMS Receptor Inhibitor II, 0.5 $mg \cdot kg^{-1}$; MCE, USA) or vehicle (carboxymethyl cellulose, CMC) for 3 consecutive days, commencing approximately one week after splenocyte transfer, coinciding with the onset of severe thrombocytopenia. Platelet counts were monitored regularly, and BM samples collected on day 16 were processed for hematoxylin-eosin staining.

Statistical Analysis

Data were analyzed using GraphPad Prism 9.0. Student's *t*-test was used for comparisons between two groups and one-way ANOVA for multiple group comparisons. All data are presented as mean ± SD. $P < 0.05$ was considered statistically significant.

Results

CSF1R is Upregulated in MKs of ITP Patients

To investigate the alterations in hematopoiesis associated with ITP, we performed scRNA-seq of BM cells from a newly diagnosed ITP patient and an HD. The ITP patient was a 65-year-old female presenting with a platelet count of 10×10^9/L and normal white blood cell and hemoglobin levels. Following quality control, dimensionality reduction and clustering analysis were conducted using UMAP and t-SNE methods (Figure 1A). Cell populations were manually annotated based on distinct gene expression patterns, including HSCs, megakaryocyte-erythroid progenitors (MEPs), MKPs, MKs, granulocytes, monocyte/macrophages, B lymphocytes, $CD4^+$ T lymphocytes, $CD8^+$ T lymphocytes, natural killer cells, and dendritic cells. Both the ITP patient and HD exhibited relatively low proportion of MKs and MKPs. Nevertheless, a marked expansion of MEPs was observed in ITP (Figure 1A), suggesting a skewing of HSC differentiation toward the erythroid lineage.

Notably, *CSF1R* expression was upregulated in MKPs from the ITP patient (Figure 1B). To validate this observation, we assessed CSF1R expression in BM-derived MKs from 26 ITP patients and 18 HDs by flow cytometry. The ITP cohort included 10 males and 16 females with a median age of 46.5 years (range: 14-74 years) and a median platelet count of 12.5 × 10^9/L (range: 1-53 × 10^9/L). MKs from ITP patients exhibited significantly higher CSF1R expression than those from HDs (Figure 1C). To determine whether altered ligand availability contributed to CSF1R upregulation, we measured concentrations of its ligands, M-CSF and IL-34, in both BM and PB supernatants. ELISA revealed no significant differences between ITP patients and HDs (Figure 1D, Figure S2), suggesting that CSF1R overexpression may be largely independent of ligand-mediated regulation. These findings implicate CSF1R as a critical contributor to impaired MK maturation in ITP and warrant further investigation into its mechanistic role in disease pathogenesis.

ITP Plasma Induces CSF1R Upregulation in Cultured MKs

To further examine the role of CSF1R in megakaryopoiesis in ITP, we employed an in vitro culture system in which $CD34^+$ HSCs were cultured with plasma derived from ITP patients or HDs (Figure S3A). Clinical characteristics of the ITP patients are summarized in Table S5. These plasma samples were used for scRNA-seq analysis and subsequent validation experiments. Cytokine profiling after ITP plasma addition revealed transient peaks of TNF-α, IFN-γ, IL-2, IL-4, IL-8, IL-10, IL-17A, IP-10, and MCP-1 within 24-48 hours, followed by a gradual decline, indicating that these factors remain biologically active between medium changes (Figure S3B). On day 4 of culture, cells exposed to plasma from a single ITP patient or a matched HD were harvested for scRNA-seq analysis. Dimensionality reduction and clustering analyses (Figure 2A) revealed a marked reduction in the proportion of MKPs and MKs in ITP compared to HD. Conversely, the ITP group exhibited an increased number of MEPs, suggesting a lineage bias toward erythropoiesis in response to ITP plasma (Figure 2B), consistent with our prior observations in patient samples. Differential gene expression analysis revealed upregulation of *CSF1R* in MKs cultured with ITP plasma in the discovery pair (Figure 2C). To validate this result, we evaluated the CSF1R expression on cultured MKs

at days 4, 7, and 10. On day 4, CSF1R expression was significantly elevated in ITP compared to HD. However, its expression declined progressively on days 7 and 10, with no significant differences observed between groups at later time points (Figure 2D). These findings indicate that CSF1R expression is transiently induced during early MK differentiation in response to ITP plasma, supporting a potential regulatory role in the impaired megakaryopoiesis observed in ITP.

CSF1R Inhibition Enhances Megakaryopoiesis in vitro

To determine whether CSF1R upregulation functionally impairs megakaryopoiesis, $CD34^+$ HSCs were cultured with plasma from ITP patients or HDs, with or without 2 μM CSF1R inhibitor. This concentration, selected from dose-optimization experiments, efficiently promoted megakaryopoiesis (Figure S4A), suppressed CSF1R between medium changes (Figure S4B), and blocked downstream signaling without inducing activation (Figure S4C). Exposure to ITP plasma markedly reduced the proportion of MKs expressing CD41a, CD42b, or CD61 at various stages of differentiation. This inhibitory effect was fully reversed by CSF1R inhibition (Figure 3A). No significant differences were observed in the mRNA levels of CD41a, CD42b, and CD61 among the groups (Figure S4D). To further assess whether the effect of CSF1R on megakaryopoiesis is influenced by anti-glycoprotein autoantibodies, we performed additional experiments using pooled plasma from anti-glycoprotein-positive or anti-glycoprotein-negative ITP patients (Table S6). Under both conditions, CSF1R inhibition consistently promoted megakaryopoiesis (Figure S5A-B), suggesting that its effect may be independent of anti-glycoprotein antibody status.

We next assessed MK ploidy distribution and platelet production. MKs cultured with ITP plasma exhibited a higher proportion of low-ploidy cells (4N: 33.10% ± 2.30% vs. 25.97% ± 2.16%, $p = 0.032$) and a significant reduction in high-ploidy MKs (≥ 16N: 27.43% ± 1.04% vs. 38.49% ± 1.02%, $p = 0.002$) (Figure 3B), accompanied by reduced in platelet release (Figure 3C). In contrast, CSF1R inhibition restored normal ploidy distribution (≥16N: 38.81% ± 0.95% vs. 27.43% ± 1.04%, $p = 0.003$) and significantly rescued platelet production (126,296 ± 10,035 vs. 63,122 ± 4,277, $p = 0.015$) (Figure 3B-C).

Confocal fluorescence microscopy further revealed a reduced number of $CD41^+$ MKs in ITP cultures, characterized by smaller cell size and absence of cytoplasmic extensions. In contrast, CSF1R inhibition markedly increased the number of $CD41^+$ MKs, which displayed enlarged cell bodies, multinucleated nuclei, irregular membrane contours, and pseudopod-like cytoplasmic protrusions, all indicative of proplatelet formation (Figure 3D).

Given the restorative effects of CSF1R inhibition on MK function, we next assessed whether CSF1R ligands (M-CSF and IL-34) influenced to megakaryopoiesis in ITP. Neither cytokine significantly influenced MK differentiation, suggesting that the regulatory effects of CSF1R in ITP are likely independent of its ligand levels (Figure S6). These results are consistent with our earlier observations (Figure 1D; Figure S2).

To further validate the functional role of CSF1R in MKs, we established stable Meg01 cell lines with lentiviral-mediated CSF1R knockdown (lv-shCSF1R) or overexpression (lv-oeCSF1R). Efficient knockdown and overexpression of CSF1R were confirmed by quantitative real-time PCR (qPCR) in Figure 4A-B. CSF1R knockdown significantly increased the proportions of $CD41^+$ (50.41% ± 0.15% vs. 34.47% ± 1.41%, $p < 0.001$), $CD61^+$ (62.43% ± 1.83% vs. 48.11% ± 2.35%, $p = 0.009$), and $CD41^+CD61^+$ (43.28% ± 0.82% vs. 26.94% ± 1.01%, $p < 0.001$) MKs compared with controls (Figure 4C). Conversely, CSF1R overexpression significantly reduced these populations ($CD41^+$ MKs, 46.10% ± 3.85% vs. 63.02% ± 2.28%, $p = 0.019$; $CD61^+$ MKs, 36.82% ± 2.72% vs. 59.94% ± 3.37%, $p = 0.006$; $CD41^+CD61^+$ MKs, 26.38% ± 2.75% vs. 48.35% ± 4.63%, $p = 0.015$) (Figure 4D). Polyploidy analysis further revealed that CSF1R knockdown decreased low-ploidy MKs (2N: 7.29% ± 0.59% vs. 12.45% ± 0.88%, $p = 0.008$; 4N: 19.42% ± 1.16% vs. 23.52% ± 0.59%, $p = 0.034$) and increased high-ploidy MKs (≥16N: 54.74% ± 1.43% vs. 44.98% ± 0.33%, $p = 0.003$), indicating enhanced maturation (Figure 4E). Conversely, CSF1R overexpression shifted the ploidy distribution toward less mature MKs, increasing 4N MKs (33.86% ± 0.93% vs. 28.68% ± 0.61%, $p = 0.010$) and decreasing ≥16N MKs (30.52% ± 1.19% vs. 38.78% ± 1.43%, $p = 0.011$) (Figure 4F).

Collectively, these findings underscore the pivotal role of CSF1R in MK differentiation

and maturation and highlight its potential contribution to the pathophysiology of ITP.

CSF1R Inhibition Facilitates Platelet Recovery in an Active Murine Model of ITP

Based on preliminary experiments, a CSF1R inhibitor dose of 0.5 mg·kg^{-1} was selected as the minimal effective and well-tolerated dose (Figure S7A), whereas a higher dose of 1 mg·kg^{-1} caused mortality in two mice within 24 hours, indicating potential toxicity. Therefore, a dose of 0.5 mg·kg^{-1} was used in all subsequent experiments. To investigate the in vivo role of CSF1R in ITP, an active ITP mouse model was established (Figure 5A). Platelet counts in ITP mice were significantly reduced compared with healthy controls at 8 days after the transfer of immunized splenocytes, confirming successful disease induction. Subsequently, ITP mice received the CSF1R inhibitor or vehicle control (CMC) for three consecutive days. Notably, CSF1R inhibitor-treated mice exhibited increased MK numbers in the BM (Figure 5B), along with a significant elevation in platelet counts on day 16 (891 ± 64 × 10^9/L vs. 547 ± 47 × 10^9/L, p = 0.005) and day 20 (1,007 ± 40 × 10^9/L vs. 590 ± 113 × 10^9/L, p = 0.025), compared with the CMC group (Figure 5C). Analysis of macrophage-mediated platelet clearance revealed no significant difference between CSF1R inhibitor-treated and control groups (Figure S7B). Together, these results demonstrate that CSF1R inhibition promotes megakaryopoiesis and enhances platelet recovery in ITP without affecting platelet clearance.

RUNX1 as a target of CSF1R

Our findings thus far underscore the crucial role of CSF1R in MK differentiation and maturation. To explore the downstream targets mediating this effect, we conducted RNA-seq on CD61$^+$ MKs cultured with ITP plasma (n = 3) or ITP plasma supplemented with a CSF1R inhibitor (n = 3). Differential expression analysis identified 166 genes that were significantly altered between the two groups, with 108 genes downregulated and 58 upregulated upon CSF1R inhibition. Among the upregulated transcripts, we noted a marked increase in *RUNX1*, a key transcription factor essential for megakaryopoiesis (Figure 6A-B). qPCR confirmed that RUNX1 mRNA expression was significantly elevated in MKs treated with the CSF1R inhibitor (Figure 6C). At the protein level, RUNX1 was similarly upregulated in Meg01 cells

following CSF1R knockdown (Figure 6D) and conversely downregulated upon CSF1R overexpression (Figure 6E). Collectively, these findings identify RUNX1 as a downstream target of CSF1R signaling and suggest that modulation of RUNX1 may underlie the regulatory role of CSF1R in MK development under ITP conditions.

Discussion

Recent advancements in the understanding of ITP pathophysiology and its clinical management have markedly improved patient outcomes[1, 8, 13, 31-33]. Yet, treatment resistance and relapse remain significant challenges, leading to refractory or chronic ITP that negatively impacts patients' quality of life. In this study, we report for the first time a substantial upregulation of CSF1R in MKs derived from ITP patients, as confirmed by scRNA-seq and validated in clinical BM samples. Our findings further demonstrate that CSF1R modulates megakaryopoiesis by regulating the expression of RUNX1, a key regulator of MK differentiation and maturation. These insights suggest that targeting CSF1R and its downstream signaling pathways may offer new therapeutic strategies for patients with ITP.

CSF1R is expressed at low levels in HSCs, and activation of the M-CSF/CSF1R signaling pathway promotes myeloid lineage commitment by inducing PU.1**,** a master regulator of myelopoiesis[23]. CSF1R expression is markedly increased during macrophage and monocyte differentiation, where it regulates cell survival, proliferation, migration, and chemotaxis[22]. Abnormal CSF1R expression has been closely associated with tumor progression through reprogramming macrophages within the tumor microenvironment, contributing to immune evasion, tumor growth, invasion and metastasis[34, 35]. In addition, the M-CSF/CSF1R signaling pathway is also involved in the pathogenesis of various inflammatory diseases, including rheumatoid arthritis[36], lupus nephritis[37], and chronic graft-versus-host disease[38]. CSF1R expression has also been detected in BM MKs, indicating a possible involvement in megakaryocytosis[25, 26]. It is also essential for the proliferation and viability of acute megakaryoblastic leukemia cell line MKPL-1[39]. The ROS-CSF1R signaling pathway has been shown to influence the differentiation of granulocyte-monocyte progenitors and MEPs at the common myeloid progenitor stage[40]. Our scRNA-seq analysis revealed an

increased erythroid lineage and decreased MK population in the BM of ITP patients. These observations were based on a single patient-donor pair. Further investigation is required to determine whether CSF1R directly regulates MEP lineage commitment toward erythroid versus megakaryocytic differentiation.

A previous study also reported elevated CSF1R protein expression in BM mononuclear cells of ITP patients[41]. The precise role of CSF1R in MKs and its contribution to the pathogenesis of ITP remains incompletely understood. Consistent with previous research findings[14, 42], our findings demonstrate that ITP patient plasma impaired MK development, and MK numbers were reduced in an active murine model of ITP. Inhibition or knockdown of CSF1R effectively reversed this impairment, restoring megakaryopoiesis. Moreover, inhibition of CSF1R facilitated platelet recovery in an active murine model of ITP. These findings indicate that aberrant CSF1R expression disrupts MK maturation and platelet production in ITP. Interestingly, the regulatory role of CSF1R in megakaryopoiesis in ITP appears to be independent of its ligands, M-CSF or IL-34. Their plasma levels were unchanged in ITP patients, and exogenous supplementation of these ligands had no effect on MK development in our in vitro culture system. These results collectively indicate that aberrant CSF1R expression disrupts MK maturation in ITP likely through a ligand-independent mechanism. Moreover, CSF1R inhibition effectively reversed the suppression of megakaryopoiesis induced by pooled plasma from anti-glycoprotein-positive or anti-glycoprotein-negative ITP patients, suggesting that CSF1R-mediated regulation of megakaryopoiesis may not be dependent on anti-glycoprotein antibodies. At present, the relative contributions of anti-glycoprotein antibodies versus other plasma components to CSF1R upregulation remain unclear. Future studies using plasma from additional patients or purified IgG will be necessary to elucidate the underlying mechanisms.

Our analysis of RNA-seq from ITP plasma-treated MKs revealed that CSF1R inhibition upregulated RUNX1 expression, a finding that was corroborated by qPCR and Western blot assays. RUNX1 plays a pivotal role in directing the lineage fate of MEPs. Its overexpression in primary human MEPs enhances megakaryocytic commitment, whereas its inhibition biases differentiation toward the erythroid lineage[43]. RUNX1 haploinsufficiency has been

shown to impair megakaryopoiesis by reducing MK-biased hematopoietic progenitor cells, likely through TGF-β1, which enhances phosphorylation of c-Jun N-terminal kinase and triggers inflammation-related signaling pathways that affect MK production[44]. Additional research demonstrated that silencing RUNX1 using a lentiviral short hairpin RNA (shRNA) strategy resulted in MKs with significantly defective responsiveness to agonists. When infused into immunodeficient NOD scid gamma mice, these MKs produced fewer circulating platelets, which exhibited shortened platelet lifespan compared to those transduced with a non-targeting control shRNA[45]. Germline mutations in *RUNX1* are linked to familial platelet disorder with a predisposition to myeloid malignancy, characterized by thrombocytopenia, bleeding tendencies, and increased risk of myeloid malignancy[46]. As a well-established transcription factor, RUNX1 governs MK differentiation, maturation, and platelet production[47, 48].

The interaction between *CSF1R* and RUNX1 appears to be reciprocal and biologically significant in regulating hematopoietic lineage commitment. CSF1R expression in the myeloid lineage largely hinges on prior transcriptional activity of PU.1, and both CSF1R and PU.1 are known direct targets of RUNX1[49]. Intriguingly, in BRAF-mutant melanomas, resistance to BRAF inhibitors has been associated with the upregulation of CSF1R and IL-34, which is also mediated by RUNX1. In this setting, RUNX1 downregulation suppresses CSF1R and IL-34 expression, while CSF1R knockdown or inhibition conversely leads to an increase in RUNX1 levels, suggesting a compensatory feedback loop. This feedback mechanism appears to impede melanoma cell proliferation and invasiveness[50]. Our study supports a similar regulatory mechanism in ITP, where CSF1R inhibition in the context of ITP results in RUNX1 upregulation, thereby enhancing MK maturation and differentiation. RUNX1 encodes multiple isoforms, with RUNX1b and RUNX1c being the major variants, transcribed from the P2 and P1 promoters, respectively. RUNX1b has been shown to be essential for MK differentiation[48]. In this study, we did not distinguish specific RUNX1 isoforms (RUNX1b and RUNX1c) primarily because their gene sequences are highly overlapping. Future studies using rigorously validated primers for isoform-specific qPCR or RNA-seq will be needed to clarify the distinct functions of RUNX1 isoforms in

megakaryocyte development.

In conclusion, this study identifies a novel regulatory axis between CSF1R and RUNX1 that governs megakaryopoiesis in ITP. Targeting CSF1R represents a promising therapeutic strategy to restore platelet production and improve outcomes in ITP patients.

References

1. Audia S, Mahévas M, Nivet M, Ouandi S, Ciudad M, Bonnotte B. Immune Thrombocytopenia: Recent Advances in Pathogenesis and Treatments. Hemasphere. 2021;5(6):e574.
2. Provan D, Semple JW. Recent advances in the mechanisms and treatment of immune thrombocytopenia. EBioMedicine. 2022;76:103820.
3. Audia S, Santegoets K, Laarhoven AG, et al. Fcγ receptor expression on splenic macrophages in adult immune thrombocytopenia. Clin Exp Immunol. 2017;188(2):275-282.
4. Li J, van der Wal DE, Zhu G, et al. Desialylation is a mechanism of Fc-independent platelet clearance and a therapeutic target in immune thrombocytopenia. Nat Commun. 2015;6:7737.
5. Tao L, Zeng Q, Li J, et al. Platelet desialylation correlates with efficacy of first-line therapies for immune thrombocytopenia. J Hematol Oncol. 2017;10(1):46.
6. Zhang F, Chu X, Wang L, et al. Cell-mediated lysis of autologous platelets in chronic idiopathic thrombocytopenic purpura. Eur J Haematol. 2006;76(5):427-431.
7. Qiu J, Liu X, Li X, et al. CD8(+) T cells induce platelet clearance in the liver via platelet desialylation in immune thrombocytopenia. Sci Rep. 2016;6:27445.
8. Cooper N, Ghanima W. Immune Thrombocytopenia. N Engl J Med. 2019;381(10):945-955.
9. Machlus KR, Italiano JE Jr. The incredible journey: From megakaryocyte development to platelet formation. J Cell Biol. 2013;201(6):785-796.
10. Khodadi E, Asnafi AA, Shahrabi S, Shahjahani M, Saki N. Bone marrow niche in immune thrombocytopenia: a focus on megakaryopoiesis. Ann Hematol. 2016;95(11):1765-1776.
11. Zeng Q, Zhu L, Tao L, et al. Relative efficacy of steroid therapy in immune thrombocytopenia mediated by anti-platelet GPIIbIIIa versus GPIbα antibodies. Am J Hematol. 2012;87(2):206-208.
12. Peng J, Ma SH, Liu J, et al. Association of autoantibody specificity and response to intravenous immunoglobulin G therapy in immune thrombocytopenia: a multicenter cohort study. J Thromb Haemost. 2014;12(4):497-504.
13. Li J, Sullivan JA, Ni H. Pathophysiology of immune thrombocytopenia. Curr Opin Hematol. 2018;25(5):373-381.
14. McMillan R, Wang L, Tomer A, Nichol J, Pistillo J. Suppression of in vitro megakaryocyte production by antiplatelet autoantibodies from adult patients with chronic ITP. Blood. 2004;103(4):1364-1369.
15. McMillan R, Nugent D. The effect of antiplatelet autoantibodies on megakaryocytopoiesis. Int J Hematol. 2005;81(2):94-99.
16. Yang L, Wang L, Zhao CH, et al. Contributions of TRAIL-mediated megakaryocyte apoptosis to impaired megakaryocyte and platelet production in immune thrombocytopenia. Blood. 2010;116(20):4307-4316.
17. Kuter DJ, Bussel JB, Lyons RM, et al. Efficacy of romiplostim in patients with chronic immune thrombocytopenic purpura: a double-blind randomised controlled trial. Lancet. 2008;371(9610):395-403.
18. Cheng G, Saleh MN, Marcher C, et al. Eltrombopag for management of chronic immune thrombocytopenia (RAISE): a 6-month, randomised, phase 3 study. Lancet. 2011;377(9763):393-402.
19. van Dijk WEM, Brandwijk ON, Heitink-Polle KMJ, Schutgens REG, van Galen KPM, Urbanus RT. Hemostatic changes by thrombopoietin-receptor agonists in immune thrombocytopenia patients. Blood Rev. 2021;47:100774.
20. Wang X, Li Y, Zhuang W. Safety analysis of romiplostim, eltrombopag, and avatrombopag post-market

approval: a pharmacovigilance study based on the FDA Adverse Event Reporting System. BMC Pharmacol Toxicol. 2025;26(1):46.

21. Ghanima W, Cooper N, Rodeghiero F, Godeau B, Bussel JB. Thrombopoietin receptor agonists: ten years later. Haematologica. 2019;104(6):1112-1123.

22. Stanley ER, Chitu V. CSF-1 receptor signaling in myeloid cells. Cold Spring Harb Perspect Biol. 2014;6(6).

23. Mossadegh-Keller N, Sarrazin S, Kandalla PK, et al. M-CSF instructs myeloid lineage fate in single haematopoietic stem cells. Nature. 2013;497(7448):239-243.

24. Sarrazin S, Mossadegh-Keller N, Fukao T, et al. MafB restricts M-CSF-dependent myeloid commitment divisions of hematopoietic stem cells. Cell. 2009;138(2):300-313.

25. Grabert K, Sehgal A, Irvine KM, et al. A Transgenic Line That Reports CSF1R Protein Expression Provides a Definitive Marker for the Mouse Mononuclear Phagocyte System. J Immunol. 2020;205(11):3154-3166.

26. Cortegano I, Serrano N, Ruiz C, et al. CD45 expression discriminates waves of embryonic megakaryocytes in the mouse. Haematologica. 2019;104(9):1853-1865.

27. Chu T, Hu S, Qi J, et al. Bifunctional effect of the inflammatory cytokine tumor necrosis factor α on megakaryopoiesis and platelet production. J Thromb Haemost. 2022;20(12):2998-3010.

28. Chow L, Aslam R, Speck ER, et al. A murine model of severe immune thrombocytopenia is induced by antibody- and CD8+ T cell-mediated responses that are differentially sensitive to therapy. Blood. 2010;115(6):1247-1253.

29. Ma L, Simpson E, Li J, et al. CD8+ T cells are predominantly protective and required for effective steroid therapy in murine models of immune thrombocytopenia. Blood. 2015;126(2):247-256.

30. Wang Y, Zhang J, Su Y, et al. miRNA-98-5p Targeting IGF2BP1 Induces Mesenchymal Stem Cell Apoptosis by Modulating PI3K/Akt and p53 in Immune Thrombocytopenia. Mol Ther Nucleic Acids. 2020;20:764-776.

31. Liu XG, Hou Y, Hou M. How we treat primary immune thrombocytopenia in adults. J Hematol Oncol. 2023;16(1):4.

32. Al-Samkari H. 2025 update on clinical trials in immune thrombocytopenia. Am J Hematol. 2024;99(11):2178-2190.

33. Chen Y, Xu Y, Li H, et al. A Novel Anti-CD38 Monoclonal Antibody for Treating Immune Thrombocytopenia. N Engl J Med. 2024;390(23):2178-2190.

34. Noy R, Pollard JW. Tumor-associated macrophages: from mechanisms to therapy. Immunity. 2014;41(1):49-61.

35. Tomassetti C, Insinga G, Gimigliano F, et al. Insights into CSF-1R Expression in the Tumor Microenvironment. Biomedicines. 2024;12(10).

36. Garcia S, Hartkamp LM, Malvar-Fernandez B, et al. Colony-stimulating factor (CSF) 1 receptor blockade reduces inflammation in human and murine models of rheumatoid arthritis. Arthritis Res Ther. 2016;18:75.

37. Bloom RD, Florquin S, Singer GG, Brennan DC, Kelley VR. Colony stimulating factor-1 in the induction of lupus nephritis. Kidney Int. 1993;43(5):1000-1009.

38. Alexander KA, Flynn R, Lineburg KE, et al. CSF-1-dependant donor-derived macrophages mediate chronic graft-versus-host disease. J Clin Invest. 2014;124(10):4266-4280.

39. Gu TL, Mercher T, Tyner JW, et al. A novel fusion of RBM6 to CSF1R in acute megakaryoblastic

leukemia. Blood. 2007;110(1):323-333.

40. Shinohara A, Imai Y, Nakagawa M, et al. Intracellular reactive oxygen species mark and influence the megakaryocyte-erythrocyte progenitor fate of common myeloid progenitors. Stem Cells. 2014;32(2):548-557.

41. Sun RJ, Yin DM, Yuan D, et al. Quantitative LC-MS/MS uncovers the regulatory role of autophagy in immune thrombocytopenia. Cancer Cell Int. 2021;21(1):548.

42. Chang M, Nakagawa PA, Williams SA, et al. Immune thrombocytopenic purpura (ITP) plasma and purified ITP monoclonal autoantibodies inhibit megakaryocytopoiesis in vitro. Blood. 2003;102(3):887-895.

43. Kwon N, Lu YC, Thompson EN, et al. CDK9 phosphorylates RUNX1 to promote megakaryocytic fate in megakaryocytic-erythroid progenitors. Blood. 2024;144(17):1800-1812.

44. Estevez B, Borst S, Jarocha D, et al. RUNX-1 haploinsufficiency causes a marked deficiency of megakaryocyte-biased hematopoietic progenitor cells. Blood. 2021;137(19):2662-2675.

45. Lee K, Ahn HS, Estevez B, Poncz M. RUNX1-deficient human megakaryocytes demonstrate thrombopoietic and platelet half-life and functional defects. Blood. 2023;141(3):260-270.

46. Schlegelberger B, Heller PG. RUNX1 deficiency (familial platelet disorder with predisposition to myeloid leukemia, FPDMM). Semin Hematol. 2017;54(2):75-80.

47. Ichikawa M, Asai T, Saito T, et al. AML-1 is required for megakaryocytic maturation and lymphocytic differentiation, but not for maintenance of hematopoietic stem cells in adult hematopoiesis. Nat Med. 2004;10(3):299-304.

48. Draper JE, Sroczynska P, Leong HS, et al. Mouse RUNX1C regulates premegakaryocytic/erythroid output and maintains survival of megakaryocyte progenitors. Blood. 2017;130(3):271-284.

49. Hoogenkamp M, Lichtinger M, Krysinska H, et al. Early chromatin unfolding by RUNX1: a molecular explanation for differential requirements during specification versus maintenance of the hematopoietic gene expression program. Blood. 2009;114(2):299-309.

50. Giricz O, Mo Y, Dahlman KB, et al. The RUNX1/IL-34/CSF-1R axis is an autocrinally regulated modulator of resistance to BRAF-V600E inhibition in melanoma. JCI Insight. 2018;3(14):e120422.

Figure Legends

Figure 1. CSF1R expression is increased in MKs from patients with ITP.

(A) scRNA-seq was performed on BM cells from a newly diagnosed ITP patient and a matched HD, followed by dimensionality reduction and clustering analyses using UMAP and t-SNE (n = 1). (B) Comparative analysis of transcriptional profiles revealed differential gene expression between the ITP and HD samples, with sigUp (red) indicating genes with $\log_2$ fold change ≥ 0 and sigDown (blue) indicating genes with $\log_2$ fold change ≤ 0 (n = 1). (C) CSF1R expression in BM MKs was evaluated by flow cytometry in ITP patients (n = 26) and HDs (n = 18). (D) Concentrations of CSF1R ligands (M-CSF and IL-34) were quantified in BM supernatants from ITP patients (n = 26) and HDs (n = 18) using ELISA. Data are presented as mean ± SD. *$p < 0.05$; ns, not significant. MKs, megakaryocytes; ITP, immune thrombocytopenia; scRNA-seq, single-cell RNA sequencing; BM, bone marrow; HD, healthy donor; CSF1R, colony-stimulating factor 1 receptor; M-CSF, macrophage colony-stimulating factor; IL-34, interleukin-34; BM, bone marrow.

Figure 2. CSF1R expression is upregulated in MKs Cultured with ITP Plasma.

(A). UMAP and t-SNE plots of scRNA-seq data showing cellular clusters derived from $CD34^+$ HSCs cultured for 4 days with plasma from an ITP patient and a matched HD (n = 1). (B) Quantification of distinct cell populations identified by scRNA-seq (n = 1). (C) Illustrative scRNA-seq visualization of relative CSF1R expression in MKs cultured with ITP or HD plasma at day 4 in the discovery pair (n = 1). (D) Flow cytometric analysis of CSF1R expression in cultured MKs at days 4, 7, and 10. CSF1R was significantly elevated in ITP-derived MKs at day 4, but differences were not observed at later time points (n = 3). Data are presented as mean ± SD. *$p < 0.05$; ns, not significant. CSF1R, colony-stimulating factor 1 receptor; MKs, megakaryocytes; ITP, immune thrombocytopenia; scRNA-seq, single-cell RNA sequencing; HSCs, hematopoietic stem cells; HD, healthy donor.

Figure 3. CSF1R inhibition restores MK differentiation and maturation in ITP in vitro.

(A). Flow cytometric analysis of the proportion of MKs expressing CD41a, CD42b, or CD61,

derived from $CD34^+$ HSCs cultured with plasma from ITP patients or healthy donors (HDs) for 7 or 10 days, with or without CSF1R inhibitor treatment (n = 5). (B) Polyploid distribution of MKs cultured under the indicated conditions, assessed by flow cytometry on day 10 (n = 3). (C) Quantification of platelet production from cultured MKs on day 12 (n = 3). (D) Confocal microscopy of $CD41^+$ MKs cultured with ITP plasma, with or without CSF1R inhibitor (n = 3). The scale bar is 50 μm (CD41, red; α-tubulin, green; phalloidin, purple; DAPI, blue). Data are presented as mean ± SD. *p < 0.05, **p < 0.01, ***p < 0.001, ****p < 0.0001; ns, not significant.

Figure 4. Altered CSF1R Expression modulates megakaryopoiesis in Meg01 cells.

(A-B) qPCR analysis confirming CSF1R knockdown (lv-sh CSF1R) or overexpression of CSF1R (lv-oe CSF1R) in the Meg01 cells compared with respective negative controls (lv-sh NC or lv-oe NC) (n = 3). (C-D) Flow cytometric analysis of the proportion of MKs following CSF1R knockdown or overexpression (n = 3). (E-F) Polyploid distribution of Meg01 cells after modulation of CSF1R expression (n = 3). Data are shown as mean ± SD. *p < 0.05, **p < 0.01, ***p < 0.001, ****p < 0.0001. CSF1R, colony-stimulating factor 1 receptor; qPCR, quantitative real-time PCR; MK, megakaryocyte.

Figure 5. CSF1R inhibitor facilitates platelet recovery in an active murine ITP model.

(A) Schematic representation of the active ITP mouse model. (B) BM samples were collected 16 days after splenocyte transfer and stained with HE to evaluate MK numbers. The scale bar is 25 μm. Black arrows indicate MKs (n = 4). (C) Platelet counts were monitored regularly in CSF1R inhibitor-treated versus CMC-treated ITP mice (n = 4). Data represent mean ± SD. *p < 0.05, **p < 0.01, ***p < 0.001. CSF1R, colony-stimulating factor 1 receptor; ITP, immune thrombocytopenia; BM, bone marrow; HE staining, hematoxylin-eosin staining; MK, megakaryocyte; CMC, carboxymethyl cellulose.

Figure 6. CSF1R regulates megakaryopoiesis via modulation of RUNX1 expression.

(A-B) Heatmap and volcano plot illustrating differentially expressed genes between the ITP

and ITP+CSF1R$_{inh}$ groups (n = 3). (C) qPCR validation of RUNX1 mRNA expression in MKs cultured with ITP plasma or ITP+CSF1R$_{inh}$ on day 10 (n = 3). (D-E) Western blot analysis of RUNX1 protein levels in Meg01 cells following CSF1R knockdown or overexpression (n = 3). *p < 0.05, **p < 0.01, ***p < 0.001. CSF1R, colony-stimulating factor 1 receptor; ITP, immune thrombocytopenia; qPCR, quantitative real-time PCR; MKs, megakaryocytes.

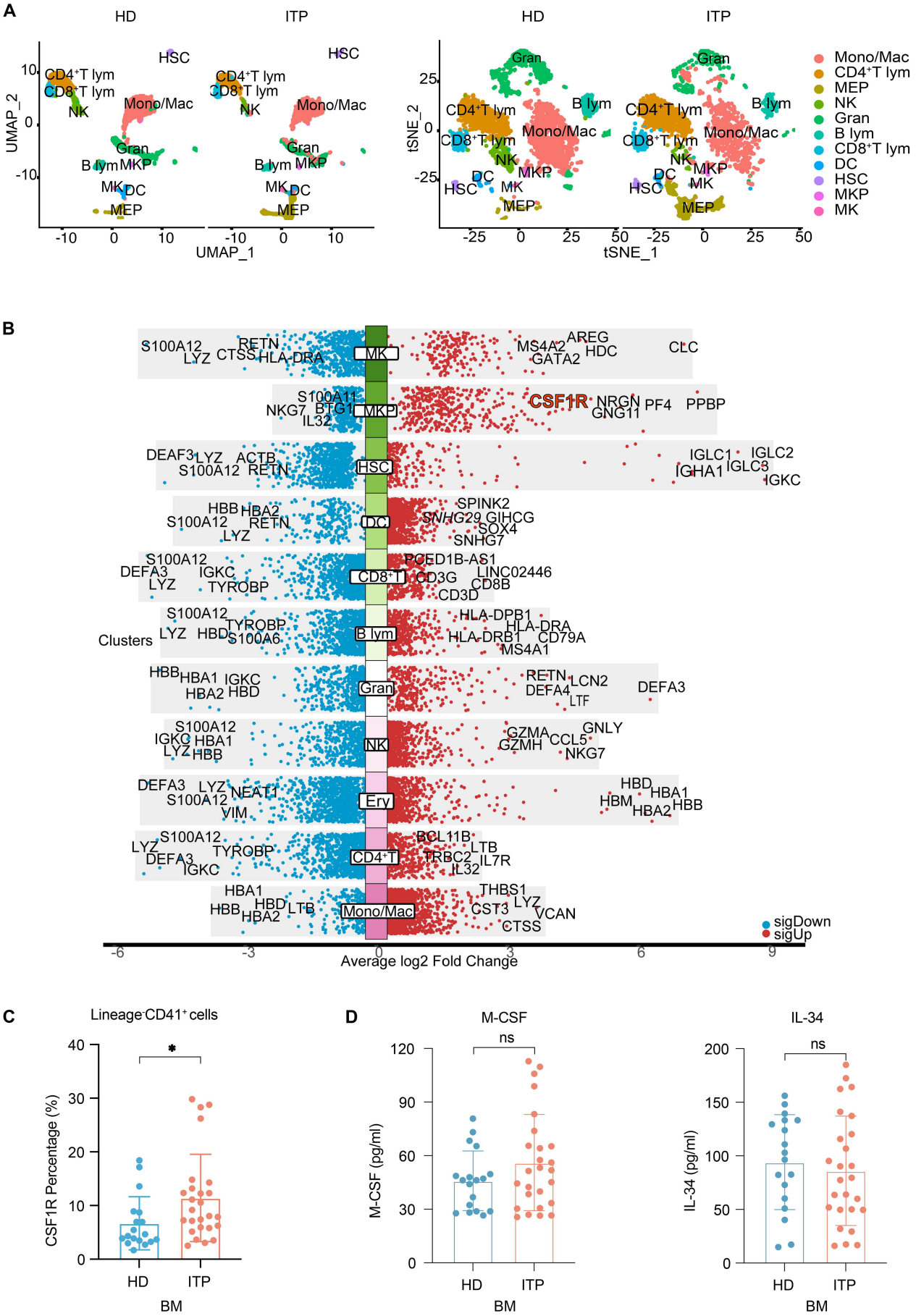
A
HD
ITP
HD
ITP
HSC
CD4+T lym
CD8+T lym
NK
Mono/Mac
Gran
B lym
MKP
MK
DC
MEP
UMAP_2
UMAP_1
tSNE_2
tSNE_1
Mono/Mac
CD4+T lym
MEP
NK
Gran
B lym
CD8+T lym
DC
HSC
MKP
MK
B
S100A12
RETN
LYZ
CTSS
HLA-DRA
MK
MS4A2
AREG
HDC
GATA2
CLC
S100A11
NKG7
BTG1
IL32
MKP
CSF1R
NRGN
GNG11
PF4
PPBP
DEAF3
LYZ
ACTB
S100A12
RETN
HSC
IGLC1
IGLC2
IGHA1
IGLC3
IGKC
HBB
HBA2
S100A12
RETN
LYZ
DC
SPINK2
SNHG29
GIHCG
SOX4
SNHG7
S100A12
DEFA3
IGKC
LYZ
TYROBP
CD8+T
PCED1B-AS1
CD3G
LINC02446
CD8B
CD3D
S100A12
TYROBP
LYZ
HBD
S100A6
Clusters
B lym
HLA-DPB1
HLA-DRA
HLA-DRB1
CD79A
MS4A1
HBB
HBA1
IGKC
HBA2
HBD
Gran
RETN
LCN2
DEFA4
LTF
DEFA3
S100A12
IGKC
HBA1
LYZ
HBB
NK
GZMA
GNLY
GZMH
CCL5
NKG7
DEFA3
LYZ
S100A12
NEAT1
VIM
Ery
HBD
HBA1
HBM
HBA2
HBB
S100A12
LYZ
TYROBP
DEFA3
IGKC
CD4+T
BCL11B
LTB
TRBC2
IL7R
IL32
HBA1
HBB
HBD
HBA2
LTB
Mono/Mac
THBS1
CST3
LYZ
VCAN
CTSS
sigDown
sigUp
-6
-3
0
3
6
9
Average log2 Fold Change
C
Lineage-CD41+ cells
CSF1R Percentage (%)
HD
ITP
BM
D
M-CSF
M-CSF (pg/ml)
ns
IL-34
IL-34 (pg/ml)
ns

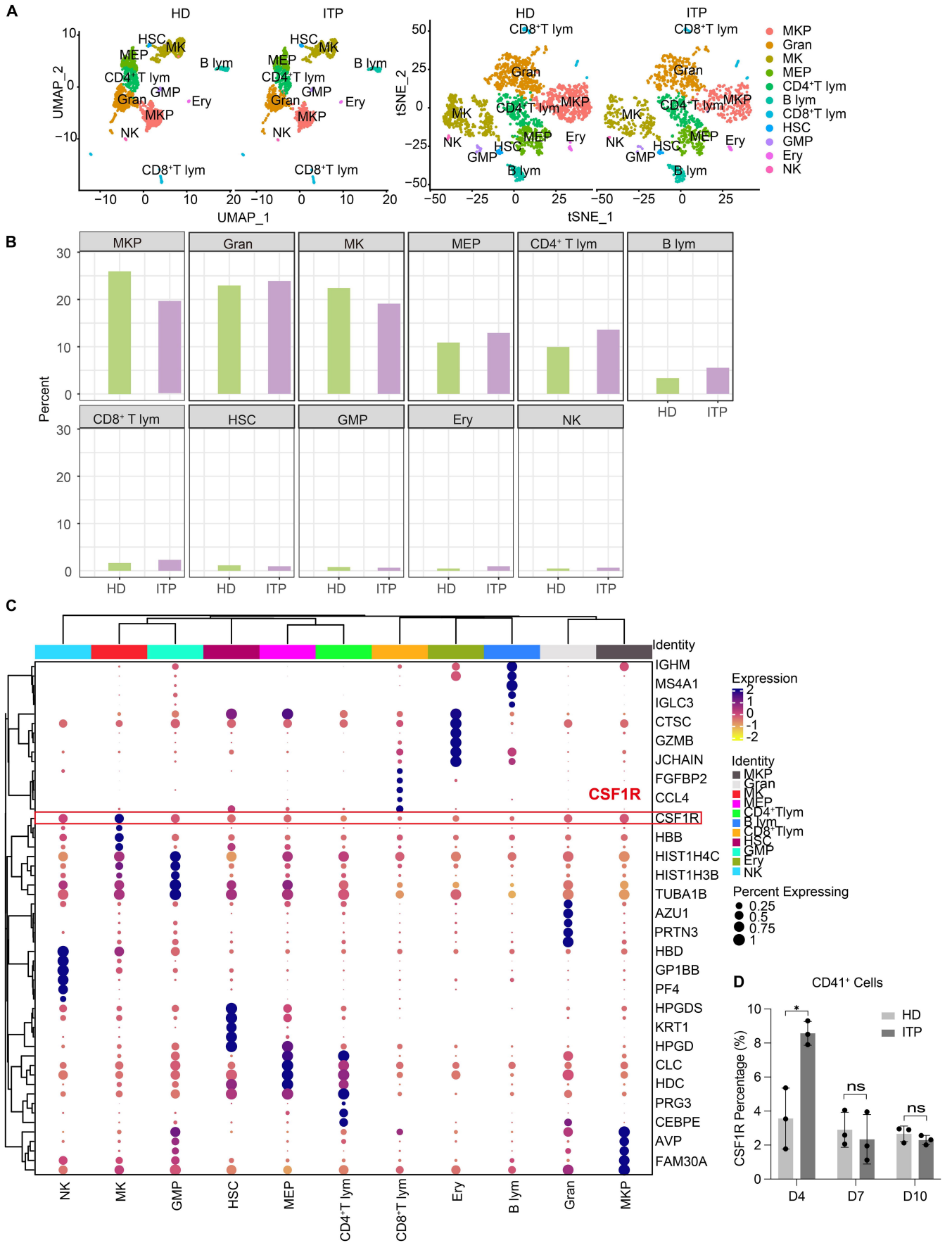
A
HD
ITP
UMAP_1
UMAP_2
tSNE_1
tSNE_2
HSC
MK
MEP
B lym
CD4⁺T lym
GMP
Gran
Ery
MKP
NK
CD8⁺T lym
MKP
Gran
MK
MEP
CD4⁺T lym
B lym
CD8⁺T lym
HSC
GMP
Ery
NK
B
Percent
CD8⁺ T lym
C
Identity
IGHM
MS4A1
IGLC3
CTSC
GZMB
JCHAIN
FGFBP2
CCL4
CSF1R
HBB
HIST1H4C
HIST1H3B
TUBA1B
AZU1
PRTN3
HBD
GP1BB
PF4
HPGDS
KRT1
HPGD
CLC
HDC
PRG3
CEBPE
AVP
FAM30A
Expression
Percent Expressing
0.25
0.5
0.75
1
D
CD41⁺ Cells
CSF1R Percentage (%)
ns
D4
D7
D10

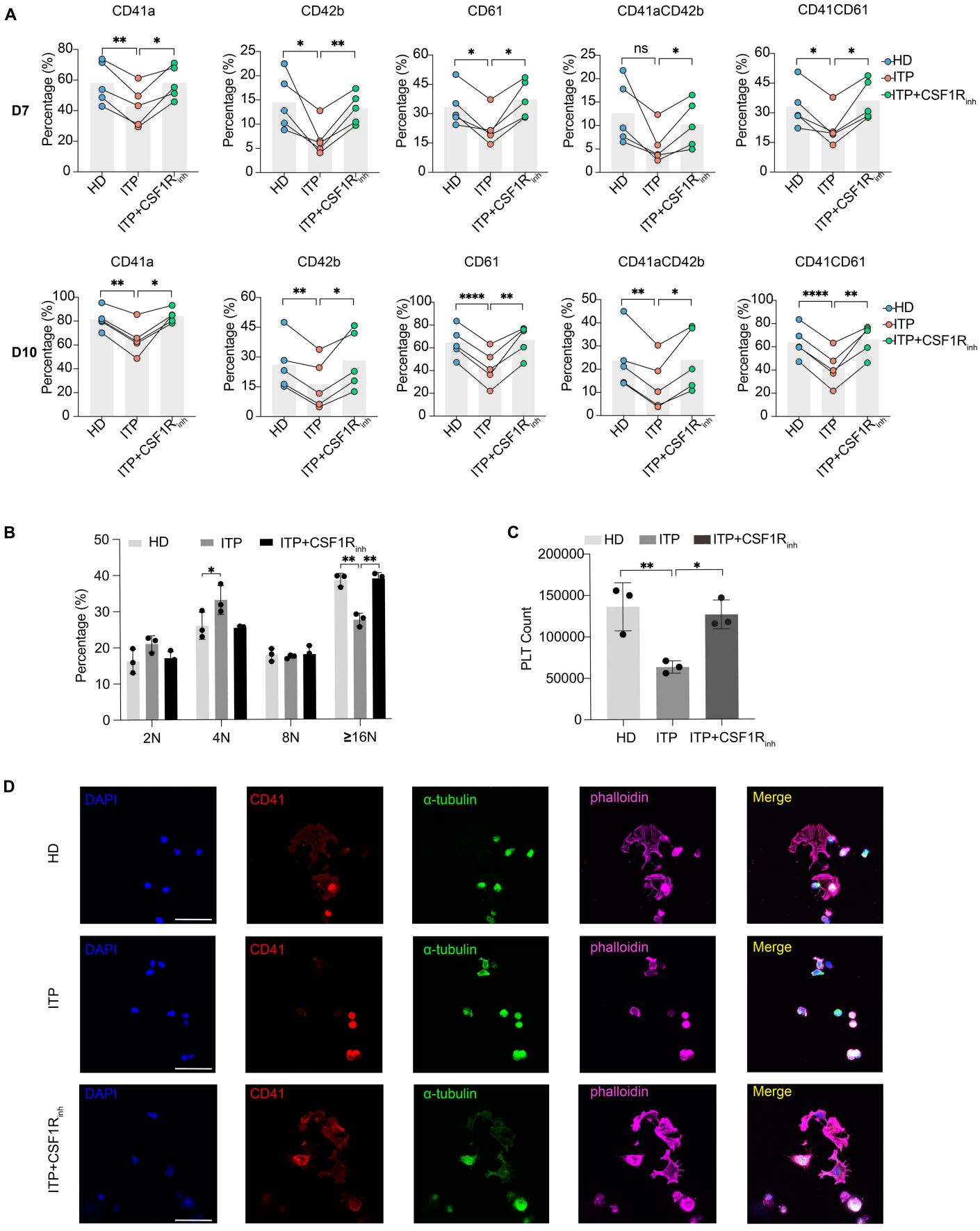
A
D7
D10
CD41a
CD42b
CD61
CD41aCD42b
CD41CD61
Percentage (%)
HD
ITP
ITP+CSF1R$_{inh}$
ns
B
2N
4N
8N
≥16N
C
PLT Count
D
DAPI
CD41
α-tubulin
phalloidin
Merge

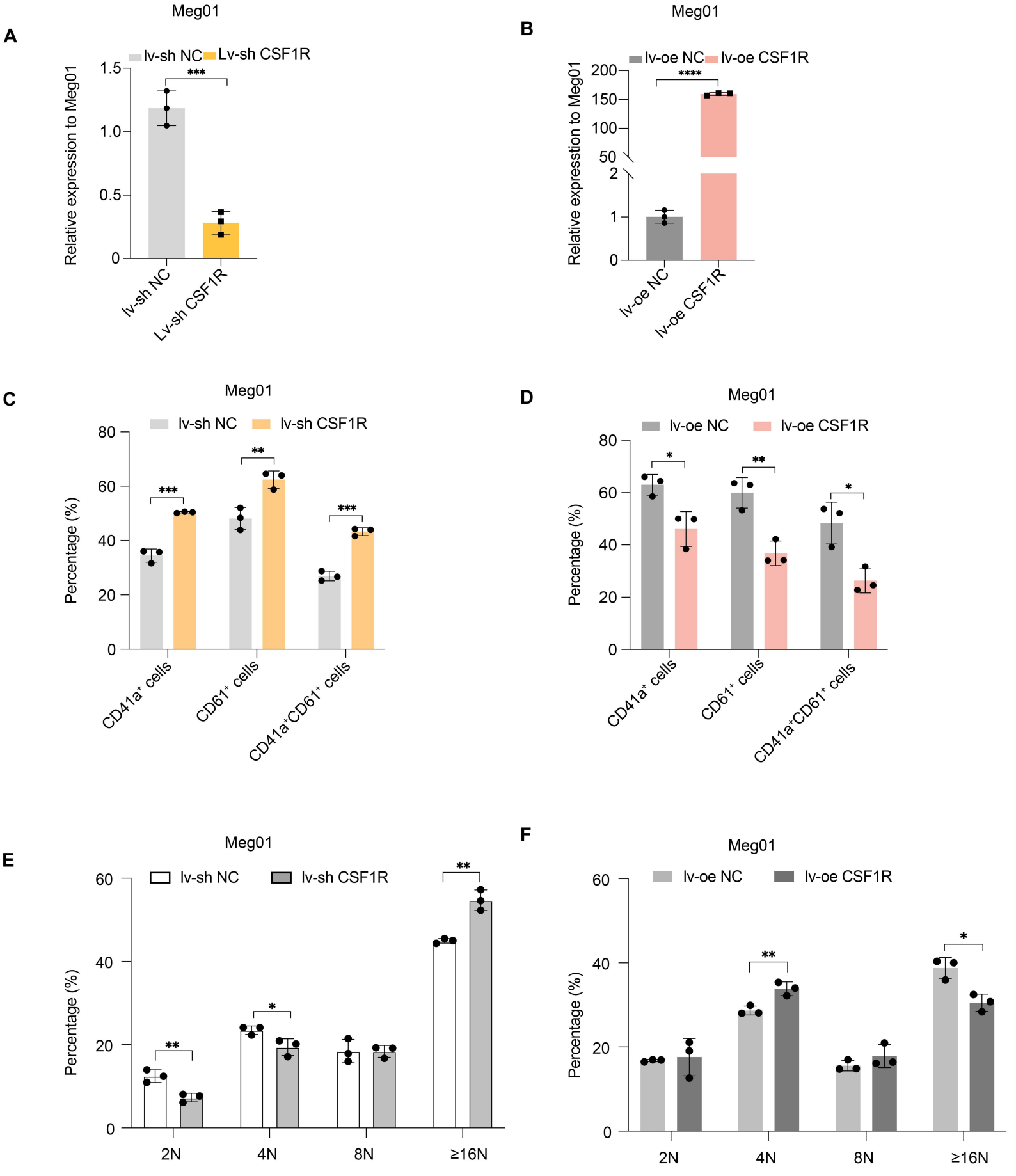
A
Meg01
lv-sh NC
Lv-sh CSF1R
Relative expression to Meg01
1.5
1.0
0.5
0
***
lv-sh NC
Lv-sh CSF1R
B
Meg01
lv-oe NC
lv-oe CSF1R
Relative expression to Meg01
200
150
100
50
2
1
0
****
lv-oe NC
lv-oe CSF1R
C
Meg01
lv-sh NC
lv-sh CSF1R
Percentage (%)
80
60
40
20
0
***
**
***
CD41a+ cells
CD61+ cells
CD41a+CD61+ cells
D
Meg01
lv-oe NC
lv-oe CSF1R
Percentage (%)
80
60
40
20
0
*
**
*
CD41a+ cells
CD61+ cells
CD41a+CD61+ cells
E
Meg01
lv-sh NC
lv-sh CSF1R
Percentage (%)
60
40
20
0
**
*
**
2N
4N
8N
≥16N
F
Meg01
lv-oe NC
lv-oe CSF1R
Percentage (%)
60
40
20
0
**
*
2N
4N
8N
≥16N

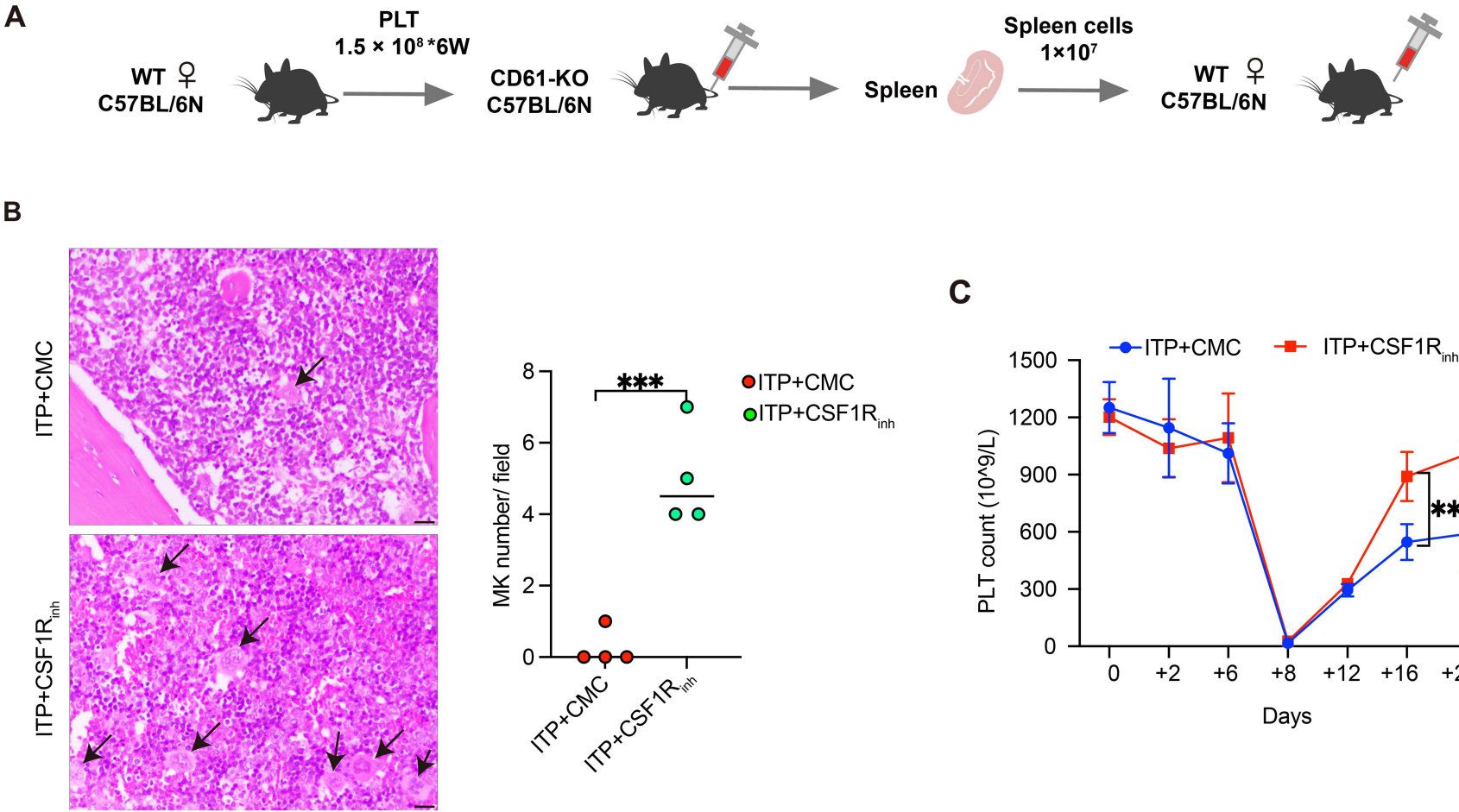
A
WT ♀
C57BL/6N
PLT
1.5 × 10⁸ *6W
CD61-KO
C57BL/6N
Spleen
Spleen cells
1×10⁷
WT ♀
C57BL/6N
B
ITP+CMC
ITP+CSF1R inh
MK number/ field
***
ITP+CMC
ITP+CSF1R inh
C
ITP+CMC
ITP+CSF1R inh
PLT count (10^9/L)
Days
0
+2
+6
+8
+12
+16
+20
**
*

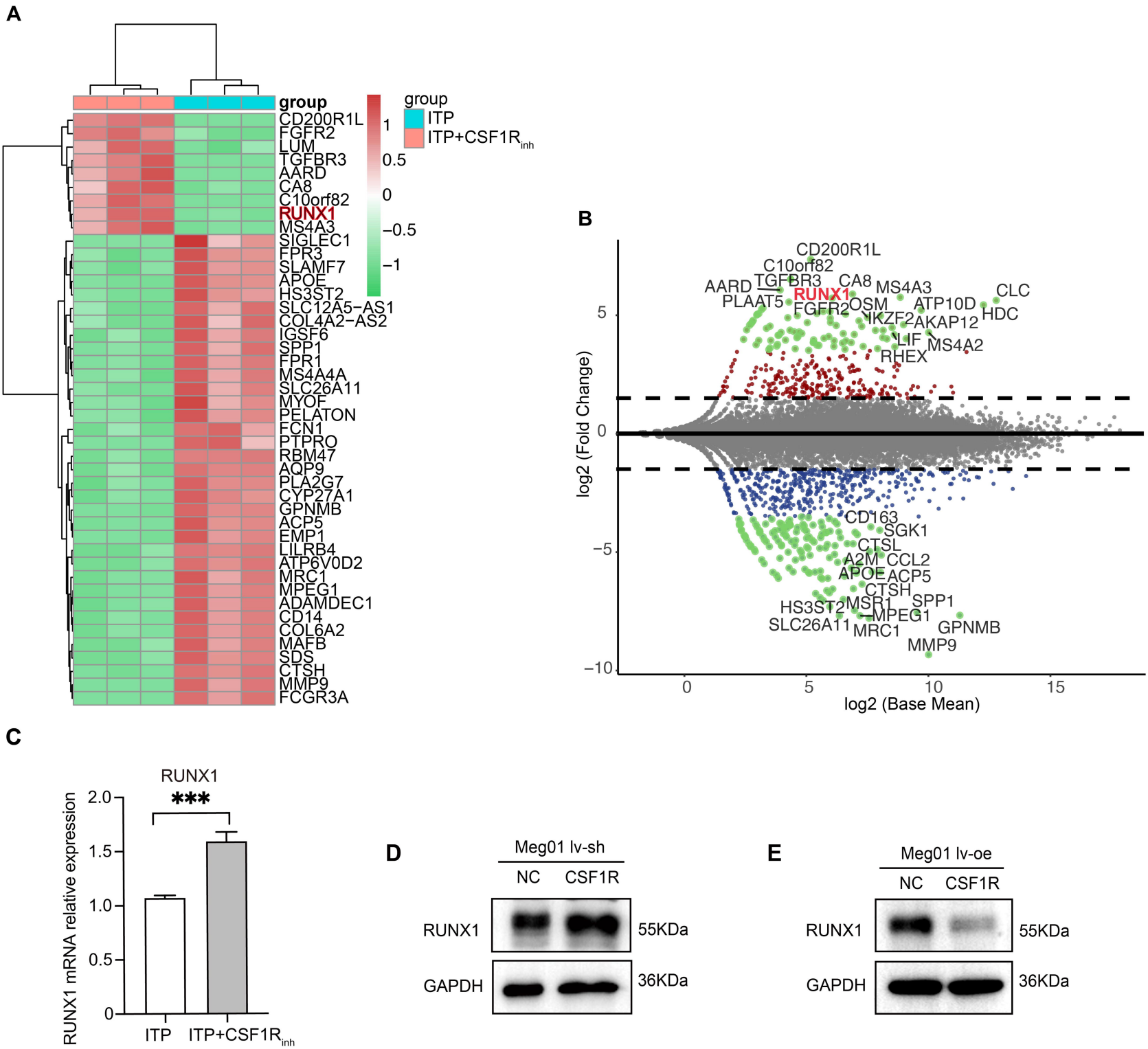
A
group
CD200R1L
FGFR2
LUM
TGFBR3
AARD
CA8
C10orf82
RUNX1
MS4A3
SIGLEC1
FPR3
SLAMF7
APOE
HS3ST2
SLC12A5−AS1
COL4A2−AS2
IGSF6
SPP1
FPR1
MS4A4A
SLC26A11
MYOF
PELATON
FCN1
PTPRO
RBM47
AQP9
PLA2G7
CYP27A1
GPNMB
ACP5
EMP1
LILRB4
ATP6V0D2
MRC1
MPEG1
ADAMDEC1
CD14
COL6A2
MAFB
SDS
CTSH
MMP9
FCGR3A
1
0.5
0
−0.5
−1
group
ITP
ITP+CSF1R$_{inh}$
B
CD200R1L
C10orf82
AARD
TGFBR3
CA8
MS4A3
CLC
PLAAT5
RUNX1
FGFR2
OSM
ATP10D
HDC
IKZF2
AKAP12
LIF
MS4A2
RHEX
CD163
SGK1
CTSL
A2M
CCL2
APOE
ACP5
CTSH
HS3ST2
MSR1
SPP1
MPEG1
SLC26A11
MRC1
GPNMB
MMP9
log2 (Fold Change)
log2 (Base Mean)
5
0
−5
−10
0
5
10
15
C
RUNX1
***
RUNX1 mRNA relative expression
2.0
1.5
1.0
0.5
0
ITP
ITP+CSF1R$_{inh}$
D
Meg01 lv-sh
NC
CSF1R
RUNX1
55KDa
GAPDH
36KDa
E
Meg01 lv-oe
NC
CSF1R
RUNX1
55KDa
GAPDH
36KDa

Supplementary Methods

Patient Samples

Newly diagnosed ITP was defined as patients within 3 months of initial diagnosis who had recurrent thrombocytopenia confirmed on two or more occasions. Blood films were examined to exclude pseudothrombocytopenia and to assess cell morphology. Splenomegaly is uncommon, and bone marrow examination in ITP typically shows normal or increased megakaryocytes with impaired maturation. Patients with secondary thrombocytopenia, including autoimmune, hematological, congenital, gestational, drug-induced, infection-associated, or other bone marrow disorders, were excluded[1, 2].

ScRNA-seq

BM samples were obtained via iliac crest aspiration. Erythrocytes were lysed using a hemolytic solution (Solarbio, China), and the remaining cells were washed and resuspended in phosphate-buffered saline (PBS; Solarbio, China) supplemented with 0.04% bovine serum albumin (BSA; Sigma-Aldrich, Japan) to maintain cell viability. Cell viability and concentration were assessed by acridine orange/propidium iodide (AO/PI) staining, and the final cell concentration was adjusted to 1×10^6 cells/mL. Single-cell suspensions were then processed for library preparation following the manufacturer's protocol using the Chromium Next GEM Chip G Single Cell Kit (10× Genomics, Cat# 1000120) and the Chromium Next GEM Single Cell 3′ GEM, Library & Gel Bead Kit v3.1 (10× Genomics, Cat# 1000121). The process included single-cell capture and library preparation, followed by a quality control assessment of library concentration and fragment size. Qualified libraries were sequenced on the Illumina NovaSeq 6000 platform using a PE150 sequencing strategy to achieve the desired sequencing depth and resolution.

The computational pipeline included demultiplexing, alignment (reference genome and software versions), stringent cell/gene quality-control thresholds (nFeature/nCount and mitochondrial cut-offs), doublet detection, ambient RNA removal, normalization (LogNormalize with log1p or SCTransform), variable-feature selection, batch correction (if applicable), dimensionality reduction, clustering, and marker detection with multiple-testing correction. To facilitate manual cluster annotation, Table S1 provides a comprehensive signature-gene reference listing marker genes for HSC, MEP, MKP, MK, and other clusters, together with their normalized

expression values (cluster-average log-normalized or SCT-normalized) and the percentage of cells expressing each gene in each cluster.

Flow Cytometry

Flow cytometry were conducted using a NovoCyte flow cytometer (ACEA Biosciences, USA). For the detection of CSF1R on human BM-derived MKs, BM cells were labeled with a BV510-conjugated lineage antibody cocktail targeting CD3, CD14, CD16, CD19, CD20, CD56 (BioLegend, USA), an APC-conjugated CD41a antibody (BD Biosciences, USA), and a FITC-conjugated CSF1R antibody (BioLegend, USA). MKs were defined as $Lineage^{-}CD41^{+}$ cells, with the gating strategy shown in Figure S1A.

To assess MK differentiation in vitro, cultured cells were harvested on days 7 and 10 and stained with APC-conjugated CD41a antibody, FITC-conjugated CD42b antibody, and PE-conjugated CD61 antibodies (all from BD Biosciences, USA).

For ploidy analysis, cells were harvested on day 12, stained with APC-conjugated CD41a antibody (BD Biosciences, USA), fixed in cold 70% ethanol, and permeabilized overnight at 4°C. Cells were then incubated with RNase buffer (Abcam, USA) and stained with propidium iodide (BioLegend, USA) for DNA content analysis. The gating strategy is shown in Figure S1B.

Platelets derived from PBMC-induced MKs were collected on day 12 and were labeled with APC-conjugated CD41a antibody (BD Biosciences, USA) to evaluate platelet production.

ELISA

To quantify cytokine levels, the concentrations of M-CSF and IL-34 in BM and PB serum samples were measured using ELISA kits specific for M-CSF and IL-34 (Aimeng Youning, China), following the manufacturer's instructions.

Cytokine dynamics after ITP plasma addition

$CD34^{+}$ HSCs were cultured with ITP plasma for the first 4 days, and the cell culture supernatants were collected at 1, 24, 48, and 72 hours after plasma addition. Cytokine levels were measured using legendplex™ Multi-Analyte Flow Assay Kit (BioLegend, USA), following the manufacturer's instructions.

CSF1R inhibitor treatment

To optimize in vitro dosing of the CSF1R inhibitor, dose-response testing was performed at 0.5, 2, and 8 μM. A concentration of 2 μM was selected for subsequent experiments, as it effectively enhanced megakaryopoiesis while maintaining cell viability. To evaluate the inhibitor's effect on CSF1R signaling, cultured cells from ITP and ITP + CSF1R inhibitor groups were collected on day 4 for Western blot analysis. Additionally, RAW264.7 mouse macrophage cells were treated with the inhibitor and analyzed by Western blot to determine whether downstream signaling pathways were suppressed or activated.

Immunofluorescence Assay

To evaluate proplatelet formation, 24-well plates (Corning, USA) were pre-coated with fibrinogen (100 μg/mL, Sigma-Aldrich, Japan) and incubated overnight at 4°C. Cultured MKs were plated and incubated for 24 hours at 37°C. Cells were then fixed and stained with anti-human CD41 antibody (Abcam, China), anti-human β-tubulin antibody(Abcam, China), phalloidin (Abcam, China), and DAPI (Beyotime, China). Cellular morphology and proplatelet structures were observed by confocal microscopy (Leica BC SP8, Germany).

Meg01 cell culture

Meg01 cells (Bena Biotech, China) were cultured in RPMI 1640 medium (Gibco, China) supplemented with 10% fetal bovine serum (FBS; SenBeiJia, China). To investigate the role of CSF1R in megakaryopoiesis, Meg01 cells were transduced with lentiviruses (Genechem, China) for CSF1R knockdown or overexpression. Transduced cells were selected based on fluorescence tagging and puromycin resistance. Successful gene modification was confirmed by qPCR analysis.

qPCR

Total RNA was extracted from cultured MKs using TRIzol reagent (Invitrogen, USA) following the manufacturer's instructions. RNA (1000 ng) was reverse-transcribed into cDNA using the 5× All-In-One RT MasterMix (Abmgood, USA). qPCR was performed using 2× SYBR Green qPCR Master Mix (Low ROX) (Bimake, China). Primer sequences for target genes are listed in Table S7 and all primers were sourced from Genewiz (China). Gene expression levels were quantified using comparative Ct method and normalized to the housekeeping gene GAPDH.

Western Blot

Cells were lysed on ice using RIPA lysis buffer containing protease and phosphatase inhibitors (Beyotime, China). Protein concentrations were determined using a BCA Protein Assay Kit (Thermo Fisher Scientific, USA). Equal amounts of protein were subjected to SDS-PAGE and transferred to 0.2 μm PVDF membranes (Merck Millipore, USA). Membranes were blocked with 5% BSA or nonfat milk for 1 hour at room temperature, followed by incubation with primary antibodies overnight at 4°C. The following primary antibodies were used: CSF1R (Abcam, Canada), p-AKT (CST, USA), AKT (CST, USA), RUNX1/AML1 (Abcam, Canada), GAPDH (CST, USA), β-Actin (CST, USA). After washing, membranes were incubated with secondary antibodies, and signals were detected using Enhanced Chemiluminescence kit (Beyotime, China).

Optimization of CSF1R inhibitor dosing in vivo

In vivo dose optimization of the CSF1R inhibitor was performed using a passive ITP mouse model[3]. C57BL/6N WT mice received tail vein injections of anti-CD42 antibody (R300, 0.1 $\mu g \cdot g^{-1}$, Emfret, Germany) twice, 24 h apart (day 0-1) to induce thrombocytopenia, while the control group received PBS. Following model establishment, mice were randomized to receive oral CSF1R inhibitor (0.1, 0.5, or 1 $mg \cdot kg^{-1}$) or CMC vehicle once daily for 3 consecutive days (day 1-3). Peripheral blood counts were monitored to assess treatment effects. The 0.5 $mg \cdot kg^{-1}$ dose was selected as the minimal effective and well-tolerated dose, whereas 1 $mg \cdot kg^{-1}$ caused mortality in two mice within 24 h, indicating potential toxicity at higher doses.

CSF1R Inhibition on platelet clearance

To determine whether CSF1R inhibition influences macrophage-mediated platelet phagocytosis, platelets from C57BL/6N WT mice were labeled via tail vein injection with DyLight488-conjugated anti-GPIbβ IgG (1 $\mu g \cdot g^{-1}$, emfret, Germany). Mice were then randomized to receive oral CSF1R inhibitor (0.1, 0.5, or 1 $mg \cdot kg^{-1}$) or CMC vehicle once daily for 3 consecutive days. Complete blood counts were measured at 0, 24, 48, and 72 hours after the first administration to monitor platelet survival.

Supplementary Tables

Table S1 Specifically expressed genes in hematopoietic cell clusters (details in Excel file)

Table S2 Clinical characteristics of 26 newly diagnosed ITP patients

ID	Age (year)	Sex (F/M)	Source	PLT ($\times 10^9$/L)
1	56	M	BM	8
2	60	M	BM	32
3	20	M	BM	9
4	50	M	BM	9
5	71	F	BM	10
6	56	F	BM	11
7	58	M	BM	21
8	47	F	BM	37
9	35	F	BM	2
10	34	F	BM	17
11	37	F	BM	37
12	58	F	BM	36
13	29	F	BM	40
14	14	M	BM	8
15	45	F	BM	1
16	62	F	BM	24
17	64	F	BM	11
18	60	M	BM	12
19	34	M	BM	6
20	70	F	BM	18
21	33	F	BM	53
22	74	M	BM	28
23	46	F	BM	10
24	21	F	BM	13
25	45	M	BM	2
26	28	F	BM	35

M: male; F: female; PB: peripheral blood; BM, bone marrow; PLT: platelet.

Table S3 Clinical characteristics of 26 newly diagnosed ITP patients

ID	Age (year)	Sex (F/M)	Source	PLT ($\times 10^9$/L)
1	56	M	BM	8
2	60	M	BM	32
3	20	M	BM	9
4	50	M	BM	9
5	71	F	BM	10
6	56	F	BM	11
7	58	M	BM	21
8	47	F	BM	37
9	53	F	BM	39
10	56	M	BM	2
11	50	F	BM	18
12	55	M	BM	25
13	18	F	BM	21
14	63	F	BM	4
15	42	M	BM	34
16	72	F	BM	32
17	43	F	BM	4
18	58	F	BM	36
19	14	M	BM	8
20	62	F	BM	24
21	45	F	BM	1
22	34	M	BM	26
23	60	F	BM	5
24	60	M	BM	12
25	64	F	BM	11
26	56	M	BM	2

M: male; F: female; PB: peripheral blood; BM, bone marrow; PLT: platelet.

Table S4. Clinical characteristics of 30 newly diagnosed ITP patients

ID	Age (year)	Sex (F/M)	Source	PLT ($\times 10^9$/L)
1	52	M	PB	45
2	27	F	PB	45
3	49	M	PB	11
4	48	F	PB	10
5	12	F	PB	29
6	34	F	PB	44
7	18	F	PB	48
8	32	F	PB	36
9	71	M	PB	3
10	25	F	PB	33
11	17	M	PB	12
12	17	M	PB	6
13	15	M	PB	27
14	71	F	PB	12
15	50	F	PB	48
16	10	M	PB	23
17	50	F	PB	34
18	34	F	PB	31
19	72	F	PB	33
20	54	F	PB	2
21	82	M	PB	48
22	69	M	PB	26
23	77	F	PB	50
24	53	F	PB	5
25	41	F	PB	30
26	38	M	PB	6
27	52	M	PB	7
28	48	F	PB	16

29	60	M	PB	32
30	49	F	PB	3

M: male; F: female; PB: peripheral blood; BM, bone marrow; PLT: platelet.

Table S5. Clinical characteristics of the newly diagnosed ITP patients

ID	Age (year)	Sex (F/M)	PLT ($\times 10^9$/L)	platelet-associated antibody (%)	Anti-GP antibodies				Application
					anti-GPIb/IX	anti-GPIb	anti-GPIIb	anti-GPIIIa	
1	45	F	1	56.3	-	-	-	-	scRNA-seq
2	50	F	18	21.6	-	-	-	-	validation
3	60	F	5	18.6	-	+	-	+	validation
4	62	F	24	46.4	-	-	-	+	validation
5	14	M	8	26.5	-	-	-	-	validation
6	42	M	34	38.0	-	-	-	-	validation

M: male; F: female; PLT: platelet; anti-GP, anti-glycoprotein.

Table S6. Clinical characteristics of the newly diagnosed ITP patients

ID	Age (year)	Sex (F/M)	PLT ($\times 10^9$/L)	platelet-associated antibody (%)	Anti-GP antibodies			
					anti-GPIb/IX	anti-GPIb	anti-GPIIb	anti-GPIIIa
1	15	M	15	45.1	+	+	-	+
2	43	F	4	26.3	-	-	+	-
3	48	F	8	35.4	-	+	+	+
4	18	F	21	41.8	-	+	-	+
5	64	F	11	28.7	-	-	-	-
6	60	M	12	46.7	-	-	-	-
7	34	M	26	41.7	-	-	-	-
8	63	F	4	35.8	-	-	-	-

M: male; F: female; PLT: platelet; anti-GP, anti-glycoprotein.

Table S7. The primer sequences for each gene

Gene	Forward primer	Reverse primer
CD41a	TGGAACGTCCTAGAAAAGACTGA	CTTCACAGTAACGCTTGTCCC
CD42b	CTGTGAGGTCTCCAAAGTGGC	GTGAGGCGAGTGTAAGGCATC
CD61	AGTAACCTGCGGATTGGCTTC	GTCACCTGGTCAGTTAGCGT
CSF1R	TCC AAA ACA CGG GGA CCT ATC	CGG GCA GGG TCT TTG ACA TA
RUNX1	CCA CCT ACC ACA GAG CCA TCA A	TTC ACT GAG CCT CGG AAA AG
GAPDH	GTC TCC TGA CTT CAA CAG CG	ACC ACC CTG TTG CTA GCC AA

Supplementary Figure Legends

Figure S1. Gating strategy for MKs. (A) Gating strategy used to identify Lineage$^-$CD41$^+$ MKs from BM cells. (B) Gating strategy for ploidy analysis of MKs. MK, megakaryocyte; BM, bone marrow.

Figure S2. Levels of M-CSF and IL-34 were in PB supernatants measured by ELISA in ITP patients (n = 30) and HDs (n = 20). Data are shown as mean ± SD. ns, not significant. M-CSF, macrophage colony-stimulating factor; IL-34, interleukin-34, PB, peripheral blood; ITP, immune thrombocytopenia; HDs, healthy donors.

Figure S3. In vitro MK differentiation and cytokine dynamics after ITP plasma treatment. (A) Schematic representation of the in vitro MK differentiation assay. (B) Cytokine dynamics in CD34$^+$ HSC cultures treated with ITP plasma during the first 4 days of differentiation. Cytokine levels were measured at 1, 24, 48, and 72 hours after plasma addition (n = 3). Data are shown as mean ± SD. MK, megakaryocyte; ITP, immune thrombocytopenia.

Figure S4. In vitro CSF1R inhibitor dosing and signaling assessment. (A) Dose-response testing of the CSF1R inhibitor (0.5, 2, and 8 μM) to determine the optimal concentration (n = 3). (B) Western blot analysis of CSF1R in ITP and ITP + CSF1R inhibitor-treated cells on day 4 (n = 3). (C) Western blot of RAW264.7 cells showing suppression of downstream signaling (P-AKT) without activation after CSF1R inhibitor treatment (n = 3). (D) qPCR analysis of mRNA levels of CD41a, CD42b, and CD61 in cultured MKs (n = 3). Data are shown as mean ± SD. *$P < 0.05$, **$P < 0.01$, ***$P < 0.001$; ITP, immune thrombocytopenia; MK, megakaryocyte.

Figure S5. CSF1R inhibition enhances megakaryocyte differentiation in vitro. (A-B) The proportion of MKs expressing CD41a, CD42b, or CD61, derived from CD34$^+$ HSCs cultured with pooled plasma from anti-glycoprotein-positive or anti-glycoprotein-negative ITP patients for 7 or 10 days, with or without CSF1R inhibitor (n = 3). Data are shown as mean ± SD. *$P < 0.05$, **$P < 0.01$, ***$P < 0.001$; ns, not significant. HSC, hematopoietic stem cell; MK, megakaryocyte; ITP, immune thrombocytopenia.

Figure S6. Effect of CSF1R ligands (M-CSF and IL-34) on megakaryopoiesis in ITP (n = 3). Data are shown as mean ± SD. CSF1R, colony-stimulating factor 1 receptor; ITP, immune thrombocytopenia; M-CSF, macrophage colony-stimulating factor; IL-34, interleukin-34.

Figure S7. In vivo CSF1R inhibitor dosing and its effect on platelet clearance. (A) Dose-response testing of the CSF1R inhibitor (0.1, 0.5, 1 $mg \cdot kg^{-1}$) in a passive ITP mouse model to determine the optimal concentration. Administration of 1 $mg \cdot kg^{-1}$ caused mortality in two mice within 24 hours (data not quantified) (n = 3). (B) Platelet clearance assessment using DyLight488-conjugated anti-GPIbβ IgG labeled platelets (n = 3). Data are shown as mean ± SD. $*P < 0.05$.

Figure S1.

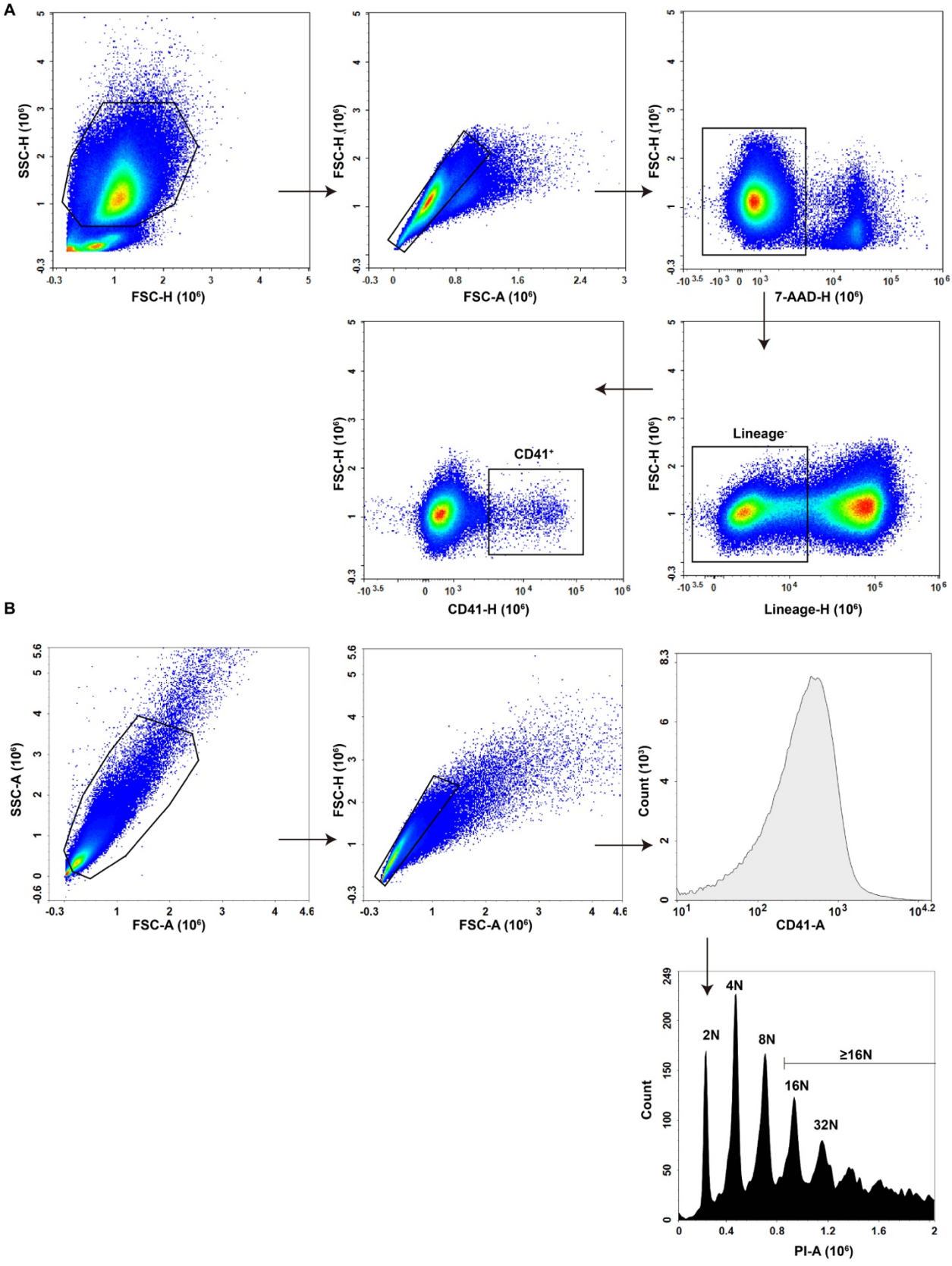
A
SSC-H (10⁶)
FSC-H (10⁶)
FSC-H (10⁶)
FSC-A (10⁶)
FSC-H (10⁶)
7-AAD-H (10⁶)
FSC-H (10⁶)
CD41⁺
CD41-H (10⁶)
FSC-H (10⁶)
Lineage⁻
Lineage-H (10⁶)
B
SSC-A (10⁶)
FSC-A (10⁶)
FSC-H (10⁶)
FSC-A (10⁶)
Count (10³)
CD41-A
Count
2N
4N
8N
16N
32N
≥16N
PI-A (10⁶)

Figure S2.

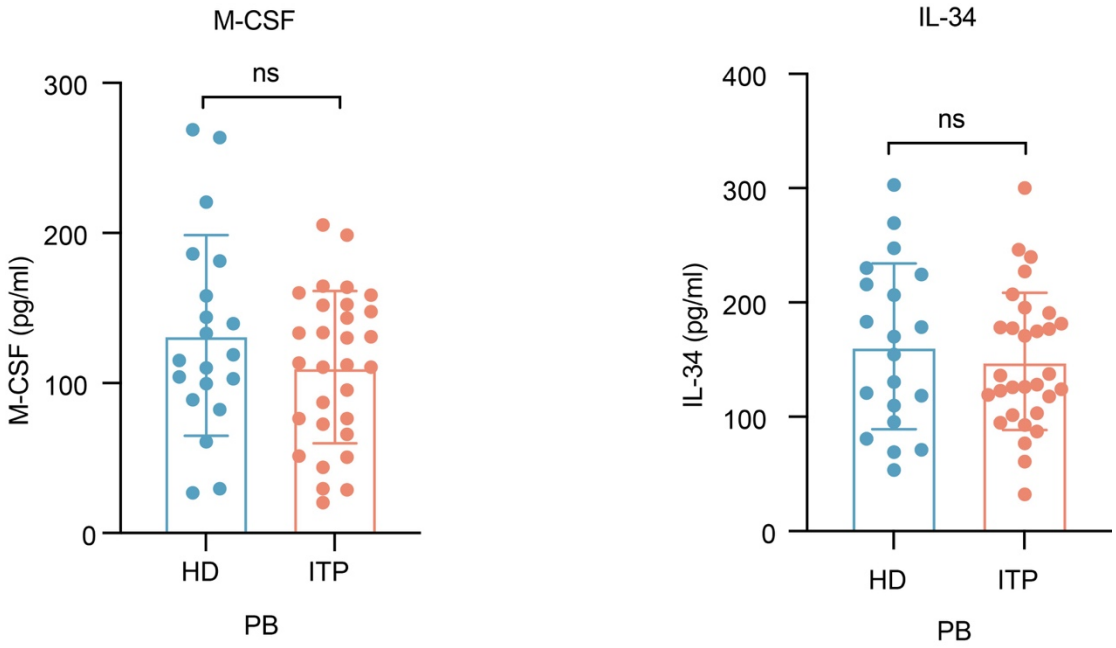
M-CSF
ns
300
200
100
0
M-CSF (pg/ml)
HD
ITP
PB
IL-34
ns
400
300
200
100
0
IL-34 (pg/ml)
HD
ITP
PB

Figure S3.

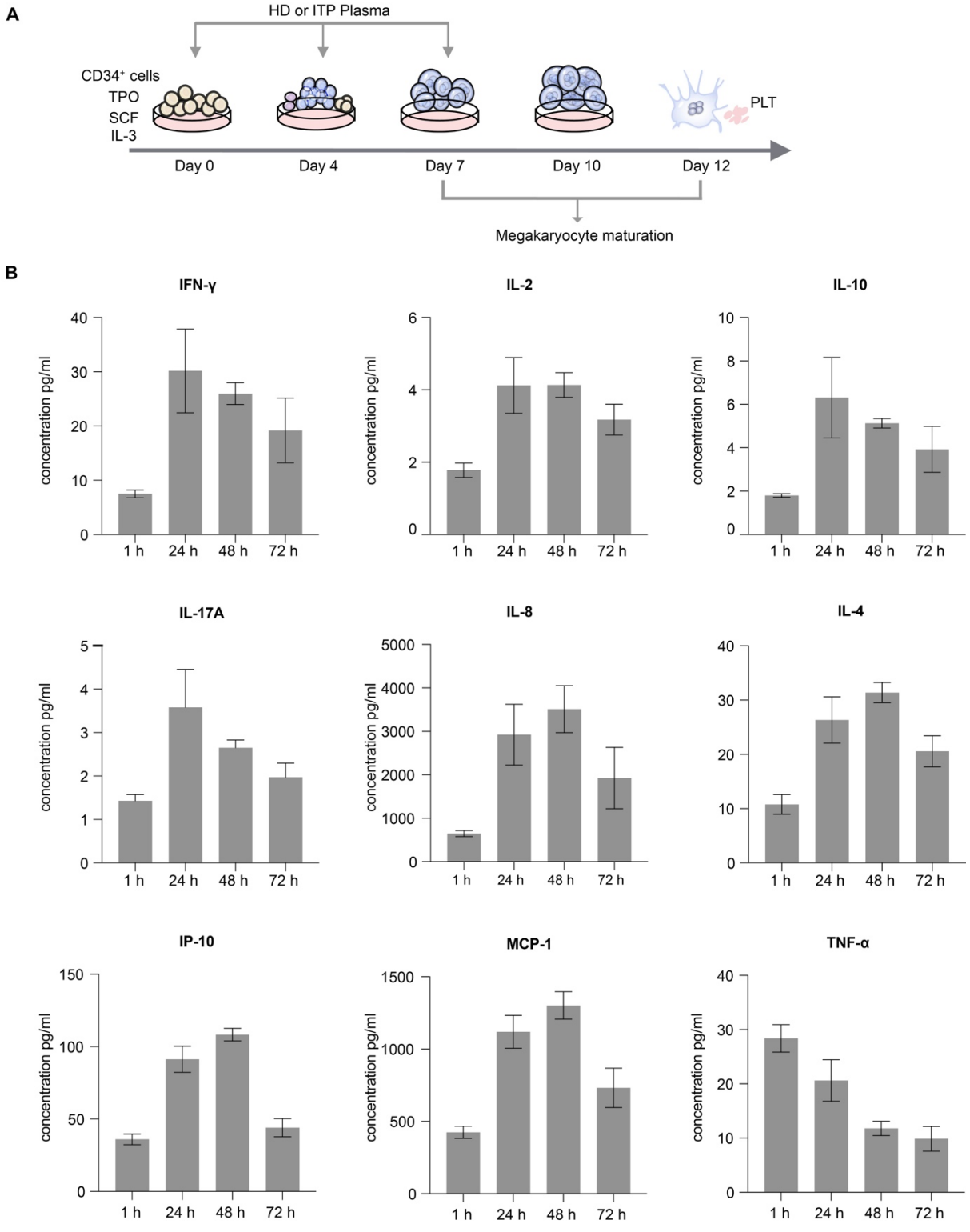
A
HD or ITP Plasma
CD34⁺ cells
TPO
SCF
IL-3
PLT
Day 0
Day 4
Day 7
Day 10
Day 12
Megakaryocyte maturation
B
IFN-γ
IL-2
IL-10
IL-17A
IL-8
IL-4
IP-10
MCP-1
TNF-α
concentration pg/ml
1 h
24 h
48 h
72 h

Figure S4.

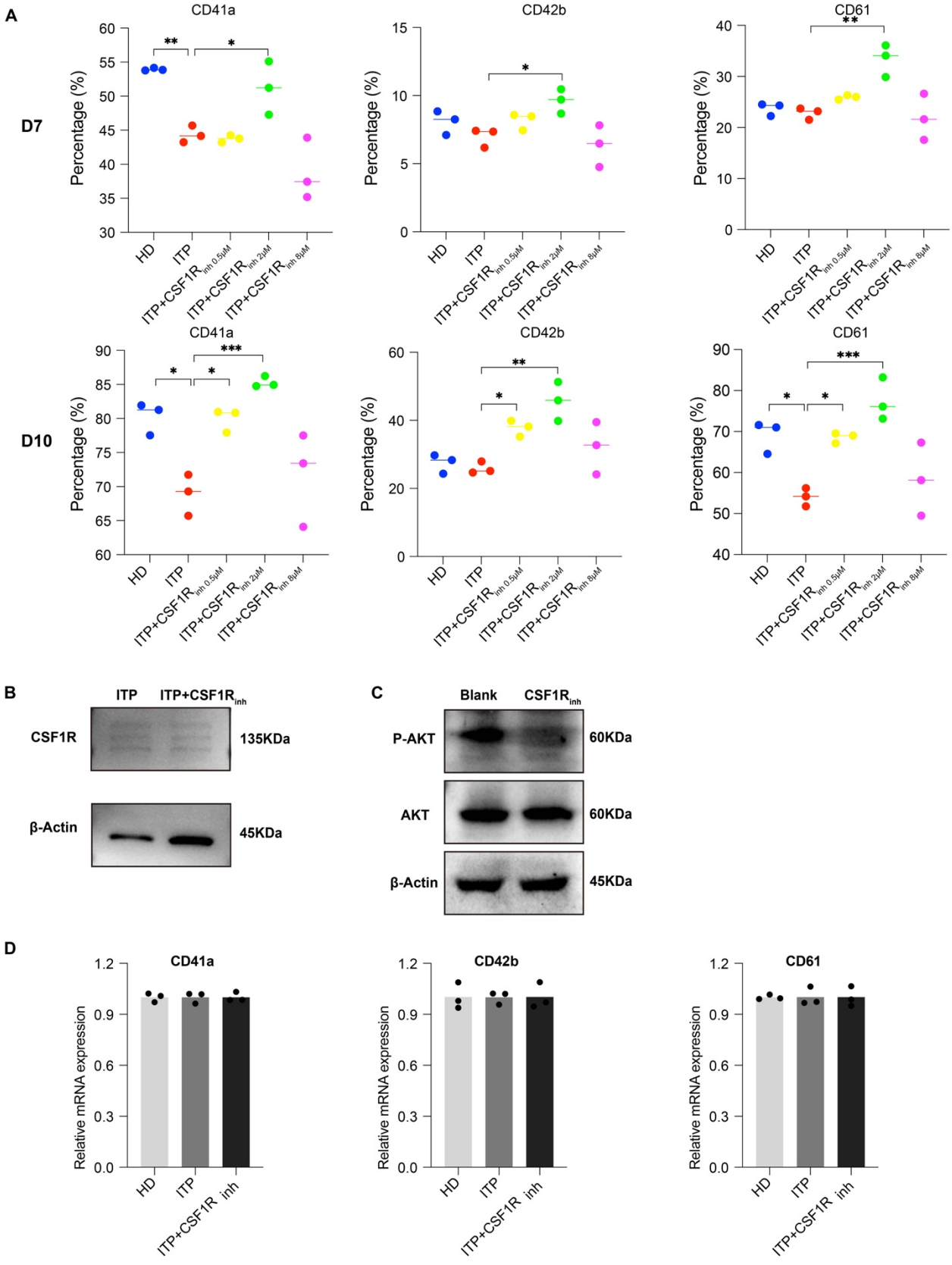
A
D7
D10
CD41a
CD42b
CD61
Percentage (%)
HD
ITP
ITP+CSF1R inh 0.5μM
ITP+CSF1R inh 2μM
ITP+CSF1R inh 8μM
B
ITP
ITP+CSF1R inh
CSF1R
135KDa
β-Actin
45KDa
C
Blank
CSF1R inh
P-AKT
60KDa
AKT
60KDa
β-Actin
45KDa
D
CD41a
CD42b
CD61
Relative mRNA expression
HD
ITP
ITP+CSF1R inh

Figure S5.

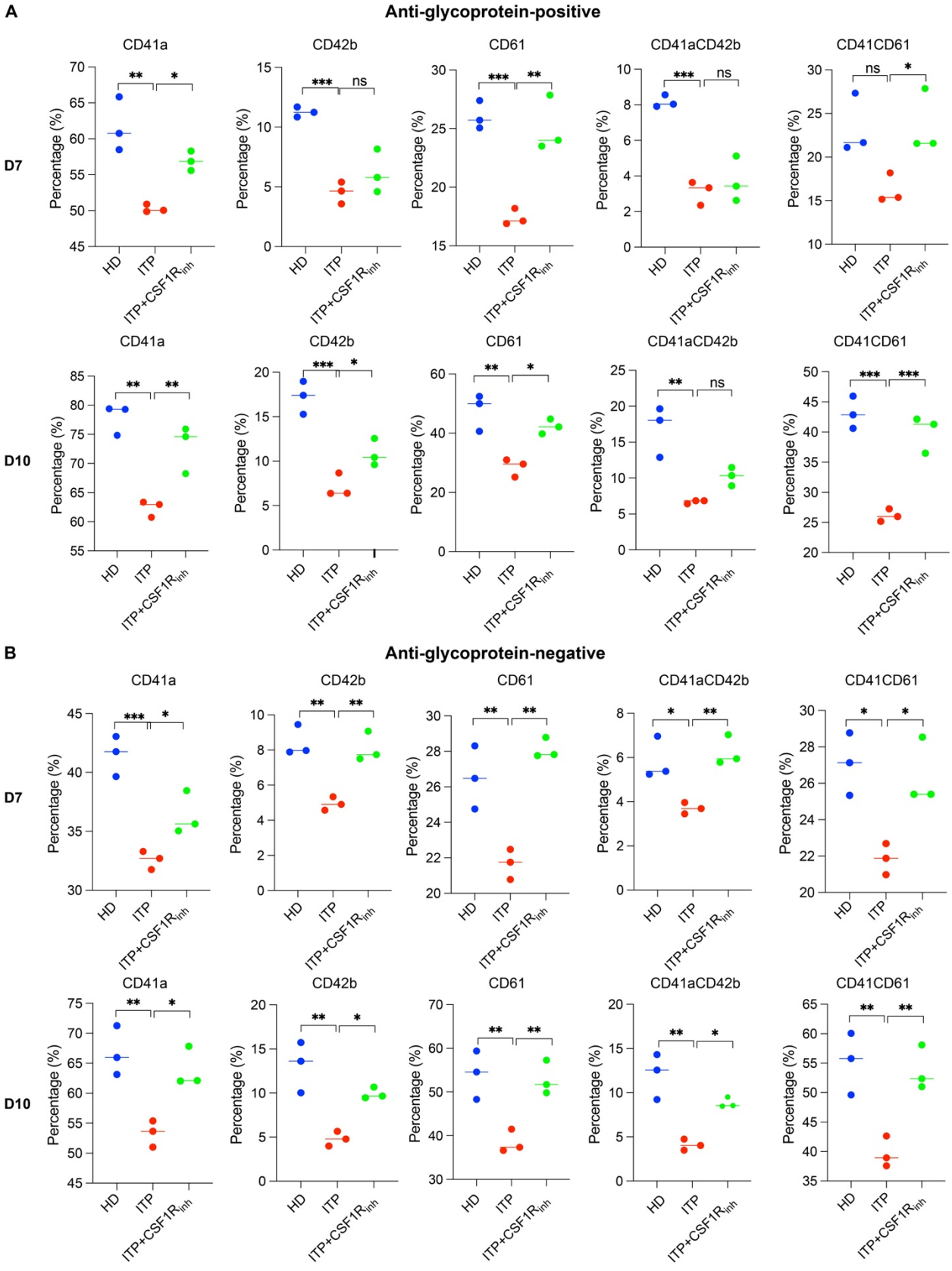
A
Anti-glycoprotein-positive
B
Anti-glycoprotein-negative
D7
D10
CD41a
CD42b
CD61
CD41aCD42b
CD41CD61
Percentage (%)
HD
ITP
ITP+CSF1R$_{inh}$
ns

Figure S6.

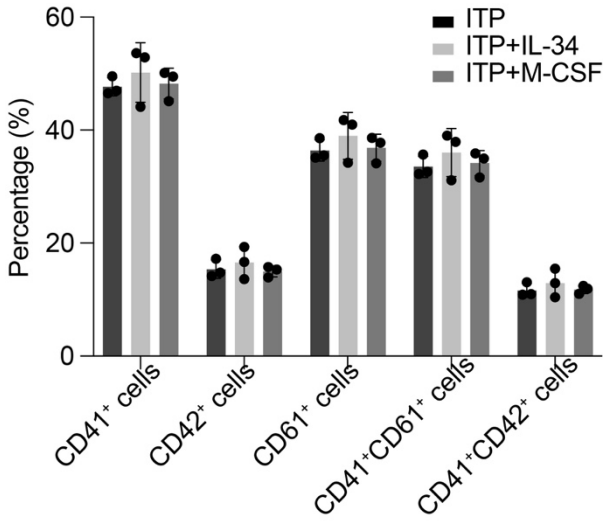
ITP
ITP+IL-34
ITP+M-CSF
Percentage (%)
60
40
20
0
CD41+ cells
CD42+ cells
CD61+ cells
CD41+CD61+ cells
CD41+CD42+ cells

Figure S7.

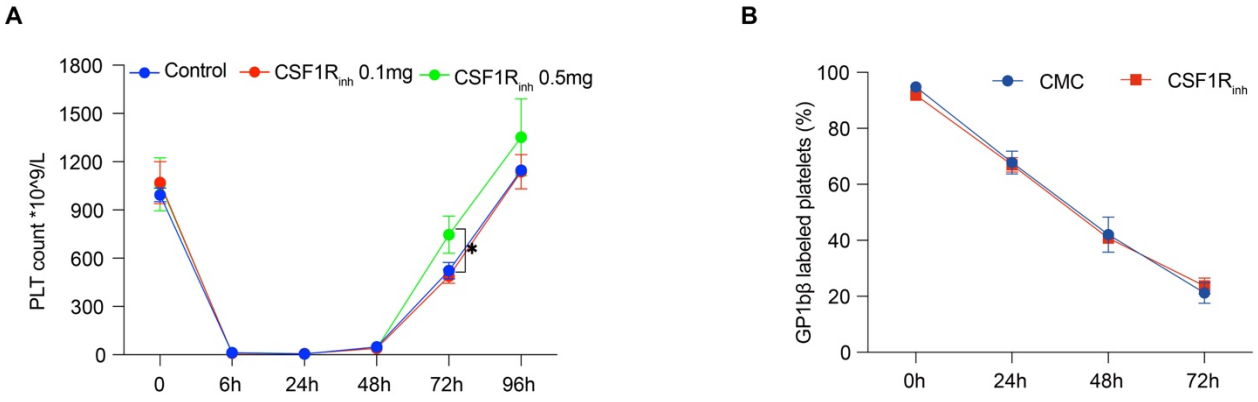
A
1800
1500
1200
900
600
300
0
PLT count *10^9/L
Control
CSF1R$_{inh}$ 0.1mg
CSF1R$_{inh}$ 0.5mg
*
0
6h
24h
48h
72h
96h
B
100
80
60
40
20
0
GP1bβ labeled platelets (%)
CMC
CSF1R$_{inh}$
0h
24h
48h
72h

References

1. [Chinese guideline on the diagnosis and management of adult primary immune thrombocytopenia (version 2020)]. *Zhonghua Xue Ye Xue Za Zhi.* 2020;41(8):617-623.

2. Liu XG, Bai XC, Chen FP, et al. Chinese guidelines for treatment of adult primary immune thrombocytopenia. *Int J Hematol.* 2018;107(6):615-623.

3. Zhang Y, Xi X, Yu H, et al. Chemically modified in-vitro-transcribed mRNA encoding thrombopoietin stimulates thrombopoiesis in mice. *Mol Ther Nucleic Acids.* 2022;29:657-671.